

IMPACT OF WET-DRY CYCLE ON MECHANICAL PROPERTIES OF EXPANSIVE
CLAY UNDER LOW OVERBURDEN STRESS

by

MD ASHRAFUZZAMAN KHAN

Presented to the Faculty of the Graduate School of
The University of Texas at Arlington in Partial Fulfillment
of the Requirements
for the Degree of

MASTER OF SCIENCE IN CIVIL ENGINEERING

THE UNIVERSITY OF TEXAS AT ARLINGTON

JULY 2016

Copyright © by MD ASHRAFUZZAMAN KHAN, 2016

All Rights Reserved



Acknowledgements

Foremost, I would like to express my sincere gratitude to Dr. Sahadat Hossain, for his valuable time, guidance, encouragement and unconditional support throughout my Master's studies. I would like to express my sincere thanks to Dr. Laureano R. Hoyos and Dr. Xinbao Yu for their willingness to serve as my committee members. I am really grateful to Dr. Sadik Khan for his constant guidance, encouragements and valuable suggestions during my stay at University of Texas at Arlington.

I would like to thank my colleagues in our research group. Particularly, I would like to thank Dr. Sonia Samir for her support and suggestions throughout my thesis work. Special thanks to Faysal and Asif for helping me during my experiments.

Finally, and most of all, I would like to thank my wife and parents for all their love, encouragement, and great support.

July 20, 2016

Abstract

IMPACT OF WET-DRY CYCLE ON MECHANICAL PROPERTIES OF EXPANSIVE CLAY UNDER LOW OVERBURDEN STRESS

MD ASHRAFUZZAMAN KHAN, MS

The University of Texas at Arlington, 2016

Supervising Professor: Sahadat Hossain

The seasonal variation in the water content termed as drying-wetting cycle is one of the most important environmental factor that may cause the degradation of strength for expansive clay. Highway embankment within the north Texas region are mostly constructed on expansive clay and shallow slope failures pose a significant maintenance problem for the Texas Department of Transportation (TxDOT). Understanding the strength loss mechanism of the expansive clay will provide some useful guidelines to design embankment with adequate factor of safety for long term drained condition. Impact of wet-dry cycle on the high plastic clay strength was measured by several researchers (Rogers and Wright, 1986; Wright et al. 2007) but the impact of wet dry cycle at low overburden stress (< 50 kPa) was not clarified, which might lead to the surficial slope failure.

In this study soil samples collected from two different slope location (DFW, Texas) with different liquid limits (LL = 40 and LL = 80) were used for the determination of shear strength parameters for 1, 3 and 5 number wet-dry cycle. Density, void ratio, moisture contents were also determined for the same number of cycles. Experimental results indicate that, for the low plastic clay changes in void ratio for the first, third and fifth cycle were 44.5%, 54.6% and 57.9% respectively. Similar trend was observed for the high plastic clay where the changes in void ratio for the first, third and fifth cycle were 44.7% ,52.0%

and 55.0% respectively. Increase in moisture content for the low plastic clay for the first, third and fifth cycles were 51.3%, 63.6% and 68.7% respectively whereas for the high plastic clay the increments were 42.6%, 52% and 56.8%. Angle of internal friction (drained condition) for the low plastic clay reduced from 33.0° to 19.3° but the cohesion increased from 2.83 kPa to 5.16 kPa after the fifth cycle. But for the high plastic clay angle of internal friction (drained condition) reduced from 28.8° to 23.0° and cohesion decreased from 4.5 kPa to 2.1 kPa, after the fifth cycle of wetting and drying.

Table of Contents

Acknowledgements	iii
Abstract	iv
List of Illustrations	ix
List of Tables	xiv
Chapter 1 Introduction.....	1
1.1 Background of the Project	1
1.2 Problem Statement.....	2
1.3 Research Objective	3
1.4 Thesis Organization.....	4
Chapter 2	5
2.1 Introduction	5
2.2 Type of Slope Failure	6
2.3 Shallow Slope Failure Mechanism	7
2.3.1 Depth of active zone in the slope	7
2.3.2 Impact of rainfall to develop a zone of saturation.....	8
2.3.3 Impact of seepage	10
2.3.4 Factor of Safety Analysis for Shallow Slope Failure	11
2.4 Impact of Wetting-Drying (w-d) cycle on the shear strength of high plasticity clay	12
2.4.1 Preparation of soil sample for wet-dry cycle	13
2.4.2 Wetting and drying procedure	14
2.4.3 Direct shear testing for wet-dry samples	15
2.4.4 Impact of wet-dry cycle on sample	15
2.4.4.1 Impact on dry density.....	15

2.4.4.2 Impact on shear strength	16
2.4.4.3 Impact on wet-dry cycle on other properties of expansive clay	18
2.5.1 Characteristics of Slope Failure in Texas.....	21
2.5.2 Geological Condition of Texas	22
2.5.3 Impact of Climate on Slope Failure	23
2.6 Measurement of Fully Softened Shear Strength	24
2.7 Empirical Correlation to Predict FSSS.....	26
2.8 Effect of sample preparation on fully softened shear strength	30
2.9 Difference between residual and fully softened friction angle	31
2.10 Use of post peak Shear Strength	33
2.11 FSSS failure envelope.....	35
2.12 Slope stability analysis with curved failure envelope.....	37
Chapter 3	39
3.1 Introduction	39
3.2 Sample Collection.....	39
3.3 Experimental Program	40
3.4 Soil Testing	41
3.4.1 Sieve Analysis	41
3.4.2 Liquid Limit and Plastic Limit	41
3.5 Direct Shear Testing.....	41
3.5.1 Compacted Sample	42
3-5-3 Fully Softened Sample.....	45
3-6 Direct Shear Test Device	46
3.7 Determination of density, moisture content and void ratio	46
Chapter 4	48

4.1 Introduction	48
4.2 Impact of wet dry cycle on basic soil parameters	49
4.2.1 Impact on moisture content	49
4.2.2 Impact on soil density	50
4.2.3 Impact on void ratio	52
4.3 Stress strain characteristic of soil under different wet-dry conditions	54
4.4 Attenuation of peak shear stress with wet-dry cycle	56
4.5 Impact of wet dry cycle on soil cohesion	58
4.6 Impact of wet dry cycle on angle of internal friction of soil	58
4.7 Impact of wet dry cycle on failure envelop	60
4.8 Determination of fully softened shear strength.....	64
4.9 Comparison of Fully Softened Shear Strength Based on Empirical Correlations	67
4.10 Factor of Safety Analysis	68
Chapter 5	72
5.1 Summary and Conclusion	72
5.2 Recommendation for Future Studies.....	75
References.....	76
Biographical Information	80

List of Illustrations

Figure 2-1 Types of Clay Movement (redrawn after Abramson et al., 2002).....	5
Figure 2-2 Failure occurred in Dallas Floodway Levee (Gamez and Stark, 2014).....	6
Figure 2-3 Seasonal water content variation with depth in unsaturated expansive soil (Lu and Likos, 2004).....	8
Figure 2-4 Rainfall Intensities capable of creating saturated conditions up to depth z_w (Pradel and Raad, 1993).....	9
Figure 2-5 Threshold permeability in clay soils for various periods of return in Los Angeles, Ventura, Orange and San Diego (Pradel and Raad,1993).....	9
Figure 2-6 Safety Factor for 2H:1V slope where a) seepage parallel to slope can develop ($\gamma = 130$ pcf) ; b) seepage parallel to slope can not develop ($\gamma = 130$ pcf) (Pradel and Raad ,1993)	10
Figure 2-7 Surficial stability analysis by total unit weights and water pressures: (a) force acting on soil block and (b) resultant forces parallel to soil slope with inclination α (Lade, 2010)	12
Figure 2-8 Direct shear chamber for wetting and drying of sample prepared by Rogers and Wright (1986)	14
Figure 2-9 Impact of wet-dry cycle on dry density by Rogers and Wright (1986).....	16
Figure 2-10 Change in Failure Envelope with Wet-Dry Cycle (Rogers, 1986).....	17
Figure 2-11 Comparison of Wet-Dry Sample Strength with Fully Softened Condition (Wright, 2007)	17
Figure 2-12 Swell Collapse behavior of sample under wet-dry cycle (Zubaydi ,2011).....	19
Figure 2-13 Shear characteristics of clays (proposed by Skempton, 1970 and redrawn by Castellanos, 2014)	20

Figure 2-14 Idealized Clay Behavior (proposed by Skempton, 1970 and redrawn by Castellanos, 2014)	20
Figure 2-15 Depth of failure of slope constructed with clay. (Castellanos, 2014)	21
Figure 2-16 Typical failure which occurs in Texas highway cut and embankment slopes (Abrams and Wright ,1972)	22
Figure 2-17 Expansive clay map of Texas.....	23
Figure 2-18 Climatic change over time (US 287, Midlothian, Texas)	24
Figure 2-19 Cracks observed at the crest of the slope at US 287, Midlothian (Sadik, 2013)	24
Figure 2-20 Relationship between the clay-size fraction and residual friction angle (Skempton 1964).....	26
Figure 2-21 Failure envelope prepared with the empirical correlations (a) for clay fraction less than 20%, (b) for clay fraction 21 to 45% and (c) for clay fraction greater than 50% as provided by Stark and Hussain (2013)	30
Figure 2-22 Secant residual friction angle relationships with liquid limit, clay-size fraction and effective normal stress	31
Figure 2-23 Shear test results for Texas soil having LL = 84; PL = 27 and Clay fraction = 53% (Castellanos, 2014).....	32
Figure 2-24 Difference between secant fully softened and residual friction angles as function of liquid limit (Stark et al. 2005)	33
Figure 2-25 Linear failure envelope obtained from direct shear test on fully softened soil with different liquid limit and clay fraction (Castellanos, 2014).	36
Figure 2-26 Schematic diagram of parameter determination for proposed power function failure criterion.....	38
Figure 3-1 Sample Locations	39

Figure 3-2 Preparation of soil samples	42
Figure 3-3 Schematic diagram of the wet-dry chamber	43
Figure 3-4 Placing of soil sample	44
Figure 3-5 Saturating the sample by adding water	44
Figure 3-6 Preparation of soil slurry for fully softened shear strength testing	45
Figure 3-7 Sample placement in direct shear box	46
Figure 4-1 Grain Size Distribution Analysis	48
Figure 4-2 Change in moisture content during wetting and drying for a) low plastic clay (LL = 40) and b) high plastic clay (LL = 80)	49
Figure 4-3 Comparison of change in moisture content for high plastic clay during wet-dry cycle	50
Figure 4-4 Change in soil density during wetting and drying for a) low plastic clay (LL = 40 and b) high plastic clay (LL =80)	51
Figure 4-5 Comparison of change in density for high plastic clay during wet-dry cycle ...	51
Figure 4-6 Change in void ratio with wet-dry cycle for a) low plastic clay (LL = 40 and b) high plastic clay (LL =80)	52
Figure 4-7 Comparison for change in void ratio for high plastic clay during wet-dry cycle	53
Figure 4-8 Direct Shear Test on Compacted Sample. a) low plastic clay (LL = 40 and b) high plastic clay (LL =80)	54
Figure 4-9 Direct Shear Test after 1 st Wet-Dry Cycle. a) low plastic clay (LL = 40 and b) high plastic clay (LL =80)	55
Figure 4-10 Direct Shear Test after 3 rd Wet-Dry Cycle. a) low plastic clay (LL = 40 and b) high plastic clay (LL =80)	55

Figure 4-11 Direct Shear Test after 5 th Wet-Dry Cycle. a) low plastic clay (LL = 40 and b) high plastic clay (LL =80)	56
Figure 4-12 Attenuation of saturated peak shear strength with wet-dry cycle. a) low plastic clay (LL = 40 and b) high plastic clay (LL =80)	57
Figure 4-13 Impact of soil wet-dry cycle on soil cohesion. a) low plastic clay (LL = 40 and b) high plastic clay (LL =80)	58
Figure 4-14 Impact of soil wet-dry cycle on internal friction of soil. a) low plastic clay (LL = 40 and b) high plastic clay (LL =80)	59
Figure 4-15 Variation of c_d and ϕ_d with respect to drying-wetting cycles (Hossain et al., 2016)	60
Figure 4-16 Direct shear test results on sample subjected to different wet-dry cycles. (a) Failure envelope for low plastic clay with LL = 40, (b) Failure envelope for high plastic clay with LL = 80	61
Figure 4-17 Change in shear strength from 1 to 3 cycle (Rogers and Wright, 1986)	62
Figure 4-18 Change in shear strength from 1 to 3 cycle (Current Study)	63
Figure 4-20 Change in shear strength from 1 to 5 cycle (Current Study)	64
Figure 4-21 Direct shear test for fully softened soil (LL = 40)	65
Figure 4-22 Direct shear test for fully softened soil (LL = 80)	65
Figure 4-23 Fully softened shear strength comparison for Eagle ford shale and soil sample collected from the DFW area.....	66
Figure 4-24 Comparison of Experimental Results with Stark and Hussain (2013), Correlation. (a) Failure envelope up to 400 kPa normal stress (b) Failure envelope up to 50 kPa	68
Figure 4-25 Factor of Safety Analysis for CL Soil (LL = 40)	69
Figure 4-26 Factor of Safety Analysis for CL Soil (LL = 80)	69

Figure 4-27 Comparison of Factor of Safety based on Fully Softened Strength 70
Figure 5-1 Impact of wet dry cycle on physical properties of CL (LL=40) soil 73
Figure 5-2 Impact of wet-dry cycle on physical properties of CH (LL=80) soil 74

List of Tables

Table 2-1 Advantages and Disadvantages of apparatus used to measure FSS (VanderBerg et al., 2013).....	25
Table 2-2 Results of slope stability analysis using different percentage of peak strength (Gregory, 2013).....	33
Table 2-3 Immerse test on compacted samples performed by Lade (2010)	37
3-1 Experimental Program	40
4-1 Soil Properties.....	48
Table 4-2 Critical Depth of Failure Based on Shallow Slope Mechanism	71
Table 5-1 Impact of wet-dry cycle on the mechanical properties of CL (LL=40) soil.....	73
Table 5-2 Impact of wet-dry cycle on mechanical properties of CH (LL =80) soil	74

Chapter 1

Introduction

1.1 Background of the Project

Fully softened shear strength refers to a condition in which the shear strength of stiff clays and shales decreases over time. This phenomenon was first observed by Skempton (1964) in the 1950s and 1960s in slopes in stiff London Clay. Skempton (1970, 1977) and others found that the fully softened strength was numerically equivalent to the peak strength of a clay in its normally consolidated state. Soil strength decreases from the compacted stage to fully softened condition with the increasing number of wet-dry cycle (Wright et al. 2007). Wet-dry cycle is regarded as the most important environmental factor that can induce damage to infrastructures such as highways and pavements (Allam and Sridharan, 1981).

Top layer (up to 10 ft) of moderate to steep slope constructed on high plasticity clay is susceptible to weathering due to wetting and drying over time (Loehr et al. ,2000). During a period of long summer with little or no rainfall will initiate surficial cracks on the slope. These surficial cracks will provide preferential flow path for the rain water to infiltrate into the slope and saturate the slope up to a certain depth. Due to cyclic wetting and drying, void ratio and moisture content will also increase (Estabragh et al., 2015). The increase in water content will decreases the effective stress cohesion intercept to zero (Bishop and Henkel, 1962). Chandler et al. (1973) and Day and Axten (1989) also reported that percolation of water into the compacted clay embankments will decrease the shear strength.

Castellanos et al. (2011), reported sixty-eight failures in stiff clays and seventy-four failures in compacted embankments related to fully softened shear strength and concluded that, application of fully softened shear strength was appropriate for the slope constructed

with liquid limits above 40 and plasticity indices above 20. Most of the soil slope constructed within the Texas are high plastic clay and liquid limit ranges in between 40 to 130 (Gregory et al. 2013). So, there is a possibility that, wet-dry cycle will reduce the shear strength of expansive clay and increase the chances of failure. Jubair (2011) also investigated the impact of wet-dry cycle on high plastic clay and concluded that, cohesion of the soil will be significantly reduced after the third cycle. Schaefer and Birchmier (2013) described the wetting and drying induced strength loss mechanism of pierre shale with a consolidation stress greater than 100 kPa. Wright et al. (2007) reported the failure envelope of Eagle Ford shale, based on nine specimens after they were subjected to 20 cycles of wetting and drying. Based on the failure envelope of Eagle Ford shale, it is observed that a stress level below 50 kPa, friction angle of the soil is much less than the friction angle calculated for higher overburden stress. When a soil is subjected to repeated wetting and drying in the laboratory, an intrinsic effective stress is imparted to it which results in greater shear strength and in a stiffer stress-strain response (Allam and Sridharan, 1981). A higher number of wet-dry cycle might increase the shear strength of soil determined from the laboratory shear testing. Based on the experimental program on expansive soil, several researchers (Tang et al., 2011, Zubaydi, 2011, Shi et al., 2013) reported that, after five wet-dry cycle expansive soil will reach an equilibrium condition.

1.2 Problem Statement

Previous researchers (Rogers and Wright, 1986; Lade, 2010; Stark and Hussain, 2013,) reported that, wet-dry cycle reduces the shear strength of soil but no clear idea was developed about the impact of liquid limit on the amount of strength reduction. Rogers and Wright (1986) conducted direct shear testing on high plastic clay specimens that went

through several wetting and drying cycles and concluded that weathering may reduce the soil cohesion to zero with a minor change in friction angle. But the back analysis of several failed slope (Wright et al, 2007) showed that, measured friction angle during the first time slide was much less than the results obtained from the experiments of wetted and dried samples or an unrealistic pore pressure parameter (r_u) value is required to obtain the factor of safety equal to unity. Rogers and Wright (1986) recommended for further laboratory investigation to observe the strength loss behavior of different clay due to wetting and drying. Though several researchers conducted triaxial and ring shear test to determine the fully softened shear strength (Wright et al,2007; Gregory and Bumpas, 2012; Castellanos, 2014), but strength loss mechanism with increasing number of wet-dry cycle were not investigated under low overburden pressure (< 50 kPa) to evaluate the shallow slope failure condition. Stark et al. (2005), Stark and Hussain (2013) provided correlation for fully softened shear strength under 50, 100 and 400 kPa normal stresses but prediction of fully softened shear strength based on their correlation is not suitable for shallow slope stability analysis where the overburden stress is expected to be lower than 50 kPa (Lade, 2010)

1.3 Research Objective

Main objective of this study is to determine the impact of wet dry cycle on change in physical and mechanical properties of expansive clay at a low overburden stress (< 50 kPa). The soil properties (including void ratio, moisture content, cohesion, angle of internal friction and modulus of elasticity) were determined for different number of wet-dry cycles.

1.4 Thesis Organization

The thesis is divided into six chapters that can be summarized as follows:

Chapter 1 provides an introduction, presents the problem statement and objective of the study.

Chapter 2 presents mechanism of shallow slope failure, impact of wet-dry cycle and development of fully softened shear strength.

Chapter 3 describes the details of work methodology for performing lab testing and development of correlation for fully softened shear strength

Chapter 4 presents the development of empirical correlations

Chapter 5 presents the results and analysis

Chapter 6 includes the summary and conclusion

Chapter 2

Literature Review

2.1 Introduction

Shallow slope failure is a common problem with the embankment constructed with high plastic clay. The reason behind the failure is the loss of shear strength with time due to weathering effects. Usually, failures occur after prolonged rainfall events which lead to the reduction of soil strength (Titi and Helwany, 2007) and most of the cases shallow slope failure varied from 3 to 6 ft depth (Loehr and Bowders, 2007). Shear strength available during the first time slide of such slope is known as “**fully softened state of strength**”, where the contribution of cohesion is almost zero and peak effective drained friction angle is the dominating parameter (Skempton 1970) and uniform mobilization of fully softened shear strength is reached along the failure surface. Shear strength parameters obtained from the direct drained shear test is not suitable for long term slope stability analysis considering the development of fully softened condition.

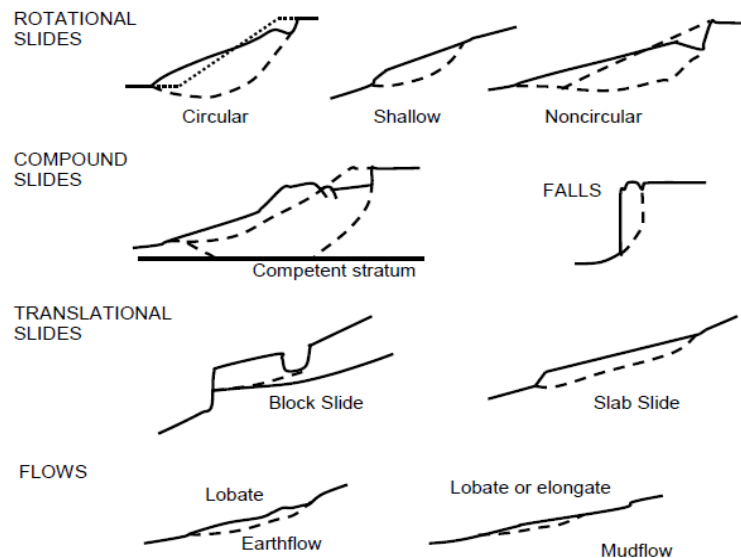


Figure 2-1 Types of Clay Movement (redrawn after Abramson et al., 2002)

2.2 Type of Slope Failure

Failure of slope may be defined as the condition when the mobilized shear strength will be just equal to the resisting or available shear strength within the soil mass through the failure surface. Types of soil, soil stratification, slope geometry and presence of water pressures are responsible for the soil movement and depth of slip surface (Titi and Helwany, 2007). Based on the depth of sliding, deep seated and shallow type of failure may occur but geometry of sliding may vary. Abramson et al. (2002) described typical slides that can occur in clay soils, such as (1) translational, (2) plane or wedge surface, (3) circular, (4) noncircular, and (5) a combination of these types. The different slope failure types are illustrated in Figure 2-1. Though there are many possible options of sliding but shallow slope failure type is predominant in north Texas region, where most of the highway slope is constructed with high Plasticity clay.



Figure 2-2 Failure occurred in Dallas Floodway Levee (Gamez and Stark, 2014)

Gamez and Stark (2014) reported some slope failure photographs for Dallas floodway levee (Figure 2-2) system where depth of slide were 2.5 m and widths from 27.5 to 36.5 m. Geotechnical design engineer working within this area should have in depth

knowledge about the shallow slope failure mechanism which is the predominant in this area.

2.3 Shallow Slope Failure Mechanism

2.3.1 *Depth of active zone in the slope*

Shallow slope failure may happen anywhere, they tend to attract more attention in semi-arid areas of the world in which the upper layer of the soil dries out for some years followed by a year with heavy rainfalls which saturate the upper layers and cause a large number of surficial failures (Lade, 2010). Change in climate might have an adverse effect on the slope. During the summer, top layer of soil dries out and longer periods of several years with little rainfall the depth of the dry soil zone increases slowly. Large surficial cracks might occur during this time which will provide a preferential flow path for the rain water. Water content varies only in the soil close to the surface and it remains relatively constant below the zone of annual fluctuation, as shown schematically in Figure 2-3. An active zone is shown in Figure 2-3 which is the evidence of a zone of relatively constant water content. The zone followed by the active zone may be considered as an impermeable layer and soil is expected to lose its cohesion within the zone of moisture variation. Just before the first time of sliding, wetting front reaches up to the maximum depth of active zone after a period of heavy rainfall and reduces the soil internal shear strength to mobilized shear. Lade (2010) concluded that, the water in the partly saturated soil below the dry soil is under tension and this provides an effective confining pressure in the partly saturated soil. Sliding failure will occur at the level of the lowest factor of safety and this is just above the depth to which the upper layer has previously dried out.

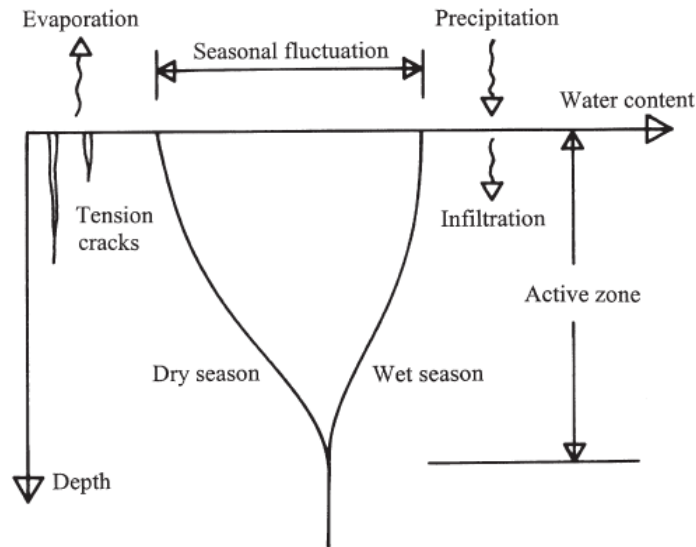


Figure 2-3 Seasonal water content variation with depth in unsaturated expansive soil (Lu and Likos, 2004)

2.3.2 Impact of rainfall to develop a zone of saturation

Rainfall is the only way to increase the moisture within the slope and creates a zone of saturation. It is possible to calculate the depth of zone of saturation using Green and Ampt model as shown in Equation 2.1. Typical diagram for rainfall intensities required to create the zone of saturation is shown in Figure 2-4.

$$T_w = \frac{\mu}{k_w} \left[z_w - S \cdot \ln \left(\frac{S+z_w}{S} \right) \right] \dots\dots\dots (2.1)$$

Where,

μ = the wettable porosity

S = the wetting front capillary suction

k_w = coefficient of permeability within the wetted zone

z_w = depth of saturation zone

T_w = time required to saturate up to depth z_w

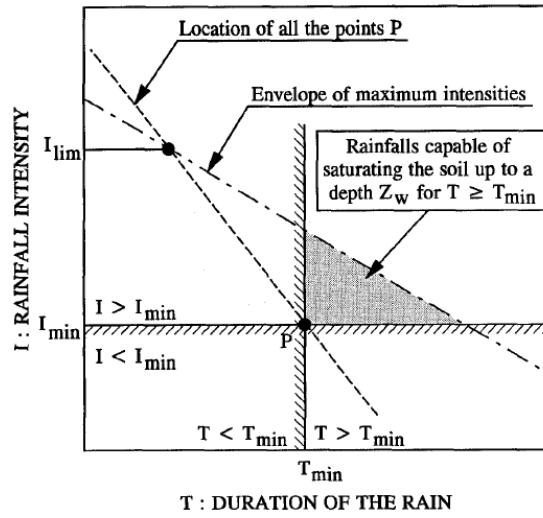


Figure 2-4 Rainfall Intensities capable of creating saturated conditions up to depth z_w
(Pradel and Raad, 1993)

period and threshold permeability. If there is no rain for a long time threshold permeability will increase. Based on rainfall analysis of four different locations in California, they observed that threshold permeability increases with the increase of return period as shown in Figure 2-5. If the return period of design rainfall increases from 10 years to 50 years, hydraulic conductivity of the wetted zone increased by almost two times.

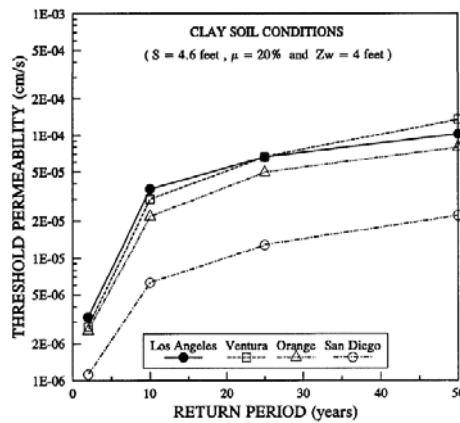


Figure 2-5 Threshold permeability in clay soils for various periods of return in Los Angeles, Ventura, Orange and San Diego (Pradel and Raad, 1993)

2.3.3 Impact of seepage

Seepage plays an important role to calculate the factor of safety of the slope. In case of shallow slope failures, it is recommended (Lade, 2010) that seepage should be considered parallel to the slope surface. Pradel and Raad (1993) presented factor of safety contour of a 2:1 slope constructed with cohesionless material having a total unit weight of 130 pcf. It is observed that, with friction angle greater than 25°, the increase in safety factor is significant. Figure 2-6a and Figure 2-6b represents the condition when seepage is parallel is possible and not possible condition.

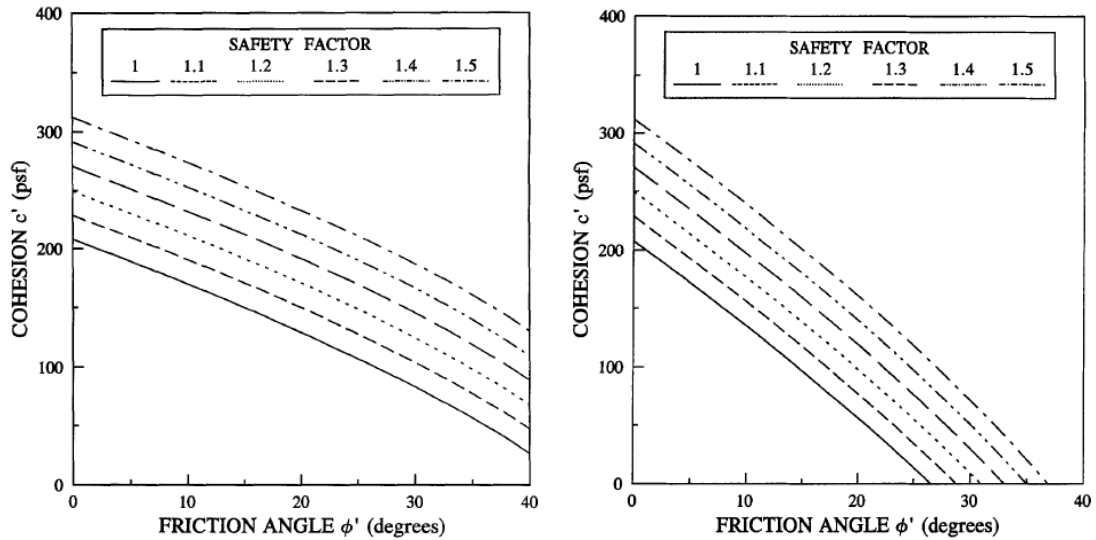


Figure 2-6 Safety Factor for 2H:1V slope where a) seepage parallel to slope can develop ($\gamma = 130$ pcf) ; b) seepage parallel to slope can not develop ($\gamma = 130$ pcf) (Pradel and Raad ,1993)

It can be concluded that, if the seepage is parallel to the slope surface, and cohesion is almost zero, it is not possible to construct a slope with 1V:2H whereas a cohesion value of 200 psf for both the cases will have a factor of safety greater than unity with zero-degree friction angle. There is a significant impact of cohesion on factor of safety if the infinite slope failure analysis is considered but normally consolidated soil, after being wetted and dried will have a zero cohesion.

2.3.4 Factor of Safety Analysis for Shallow Slope Failure

During the event of a rainfall, water enters in to the slope through the cracks and considered to be directed parallel to the surface of the slope guided by an imaginary impermeable layer. The location of the impermeable layer is the zone lied beneath the active zone of seasonal variation. It is assumed that, flow lines are parallel to the slope and the equipotential lines are perpendicular to the slope. The water pressure is therefore zero at the ground surface and it increases with depth as indicated in Figure 2-7. According to Lade (2010) factor of safety of such slope can be defined by the following equation 2.2.

$$F = \frac{S}{\tau} = \frac{c' + (\gamma_{\text{sat}} - \gamma_w) \cdot h \cdot \cos 2\alpha \cdot \tan \varphi'}{\gamma_{\text{sat}} \cdot h \cdot \cos \alpha \cdot \sin \alpha} \dots\dots\dots (2.2)$$

Where,

S = resisting shear strength

τ = mobilized shear strength

γ_{sat} = Saturated unit weight of soil

γ_w = unit weight of water

h = depth of sliding

α = slope angle

c' = cohesion

φ' = friction angle

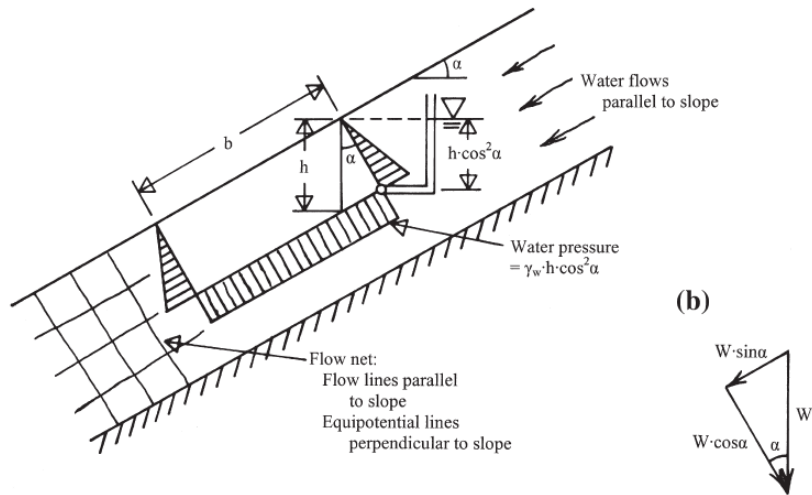


Figure 2-7 Surficial stability analysis by total unit weights and water pressures: (a) force acting on soil block and (b) resultant forces parallel to soil slope with inclination α (Lade, 2010)

Due to wetting and drying cycle cohesion reduces with time and assumed to be zero while considering fully softened shear strength. Putting $c' = 0$, equation 2.2 can be simplified as the following. So, it is possible to calculate the factor of safety just knowing the fully softened friction angle.

$$F = \frac{S}{\tau} = \frac{(\gamma_{\text{sat}} - \gamma_w) \cdot \tan \phi'}{\tan \alpha} \dots \dots \dots (2.3)$$

2.4 Impact of Wetting-Drying (w-d) cycle on the shear strength of high plasticity clay

Rogers and Wright (1986) performed a number of laboratory tests to understand the shear strength of high plastic clay used to construct embankment in Texas. They performed direct shear and triaxial tests for compacted samples as well as sample that went through various wet-dry cycle up to 30 cycles. The soil use for that research was

Beaumont clay with an average liquid limit of 70 and plastic limit of 20 percent; the average plasticity index was 50 percent. Method of soil sample preparation and testing are discussed within the sub sequent sections.

2.4.1 Preparation of soil sample for wet-dry cycle

The effect of wetting and drying were first examined on compacted specimens with a height 0.816 inches and a diameter of 2.5 inches, which were the appropriate size for the direct shear device. Soil used for preparing compacted samples were air dried, pulverized and passed through a #40 U.S. sieve. For Beaumont clay it was difficult to extrude soil sample at a moisture content less than 30 percent. After 24 hrs of curing in a humid room, moist soil was forced through the aluminum plate containing numerous 1/32 inch diameter holes. For the extrusion of soil hydraulic ram was used and extruded sample was then cut into standard 0.5 inches in length and allowed to dry approximately the desired moisture content of 24 percent for compaction. Specimen were compacted in a 2.5 inch diameter mold specially designed for compacting direct shear specimens. Values of dry density (96.3 pcf) and optimum moisture content (24 percent) based upon the Texas SDHPT Test method Tex-113-E were used to as "target" values. A 2.15 pound hammer with an acrylic cylindrical face 2.4 inches in diameter was utilized to compact the specimens with four equal lifts using six drops of hammer at a height of 12 inches. After preparation, the mold was disassembled and the specimen was placed in a stainless steel ring with an inside diameter of 2.5 inches and height of 0.816 inches.

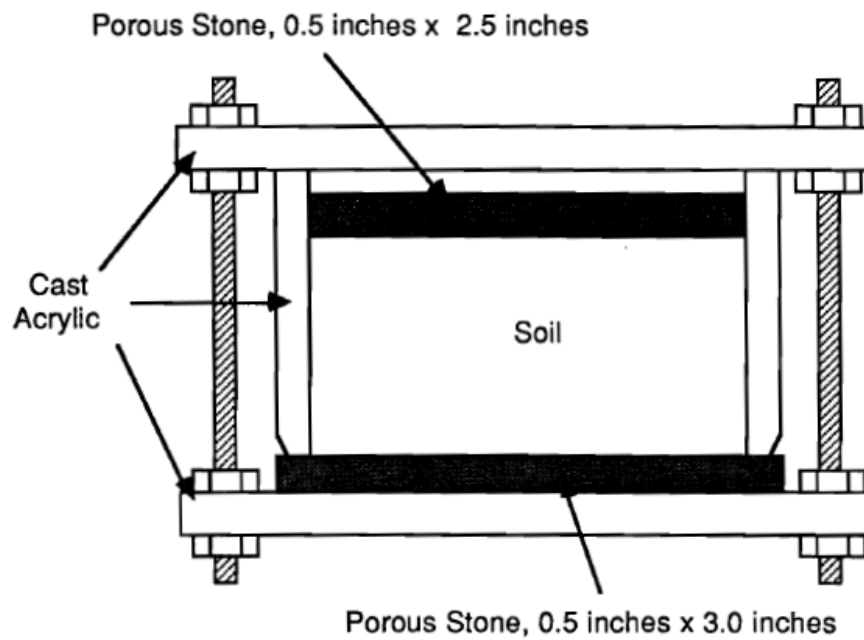


Figure 2-8 Direct shear chamber for wetting and drying of sample prepared by Rogers and Wright (1986)

2.4.2 Wetting and drying procedure

To repeat the wetting and drying procedure special chamber was required to maintain the direct shear specimen approximate shape during the wetting and drying procedure. Dimension of the chamber used by Rogers and Wright (1986) was 2.55 inches in diameter and 2.5 inch in height; this cylinder was secured between two circular acrylic end-plates with three threaded rods and nuts as shown in Figure 2-8. Two porous stones were placed at top and bottom of the chamber so that water could easily enter into the chamber. Specimens were kept in the oven in 140 degrees Fahrenheit for drying at least 24 hrs. Average decrease of moisture content of 50 percent was considered as complete drying and increase of moisture content of 50 percent of the average moisture content was

considered as full wetted sample. After wetting and drying cycle of each specimen, the specimen was extruded from the acrylic cylinder and trimmed. The specimen's dry density, degree of saturation and void ratio at the end of wetting and drying were estimated using the weight and the clay's measured specific gravity of 2.69.

2.4.3 Direct shear testing for wet-dry samples

After a desired number of wetting-drying cycles specimens were trimmed into a stainless steel ring with a diameter of 2.5 inches and a height of 0.816 inches. Finally, they were extruded from the ring into the direct shear box for testing. Specimen were consolidated vertically using a single load increment with a loaded hanger and no free water was accessible to the specimen at the onset of consolidation. Distilled water was used immediately after the application of normal load and a constant level of water was maintained throughout the test. Maximum time for completion of primary consolidation was 5.5 hrs. but a 24 hrs. period of consolidation was used during the experiment. The rate of shear was set as 0.002 inch/hrs. to ensure adequate drainage. Each specimen was sheared up to a deformation of 0.15 inches and some cases it took 5 days to reach the peak shear strength with slow shearing rate.

2.4.4 Impact of wet-dry cycle on sample

2.4.4.1 Impact on dry density

With each number of wet-dry cycle, there is a remarkable decrease in dry density. Figure 2-9 represents the impact of wet-dry cycle in dry density. Maximum change in dry density was observed just after the first wet-dry cycle and after 5th wet-dry cycle the rate of change was zero.

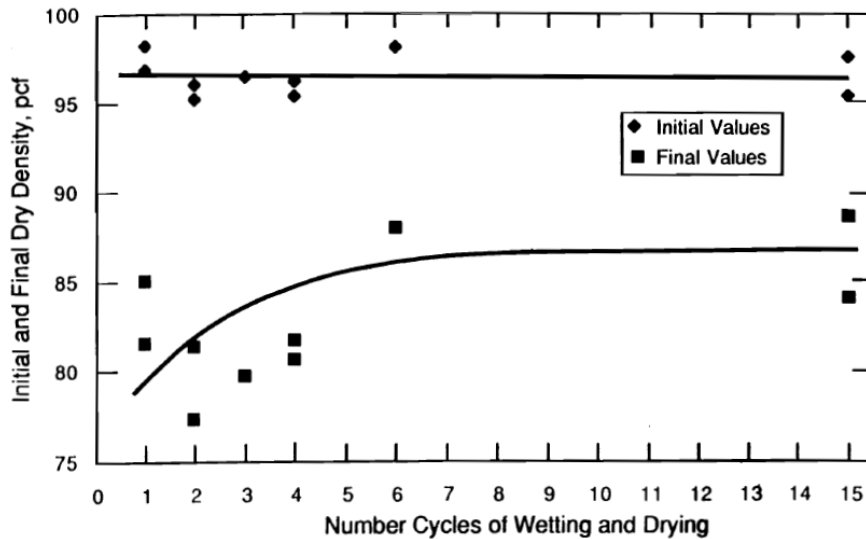


Figure 2-9 Impact of wet-dry cycle on dry density by Rogers and Wright (1986)

2.4.4.2 Impact on shear strength

Experimental results obtained by Rogers and Wright (1986), showed that, after thirty drying and wetting cycle cohesion decreases to zero. Failure envelope using different wet-dry soil samples are shown in Figure 2-10. Though there is no significant pattern of strength loss with wet-dry cycle but it is observed that, friction angle was almost similar for different samples. Experimental results obtained by Wright et al (2007) is also shown in Figure 2-11. For both cases, normal stress up to 50 kPa was used to compare the results in case of a shallow slope failure. For Eagle Ford Shale with a liquid limit of 88 was used for the preparation of wet-dry sample and also for the preparation of fully softened sample using slurry. It is observed that, wet-dry cycle reduces the shear strength and reach to the fully softening condition. After complete weathering soil specimens are considered to be fully softened with a zero value of cohesion.

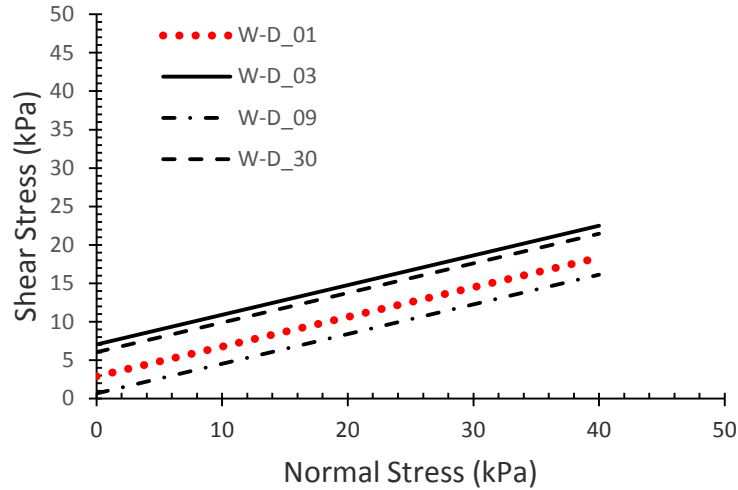


Figure 2-10 Change in Failure Envelope with Wet-Dry Cycle (Rogers, 1986)

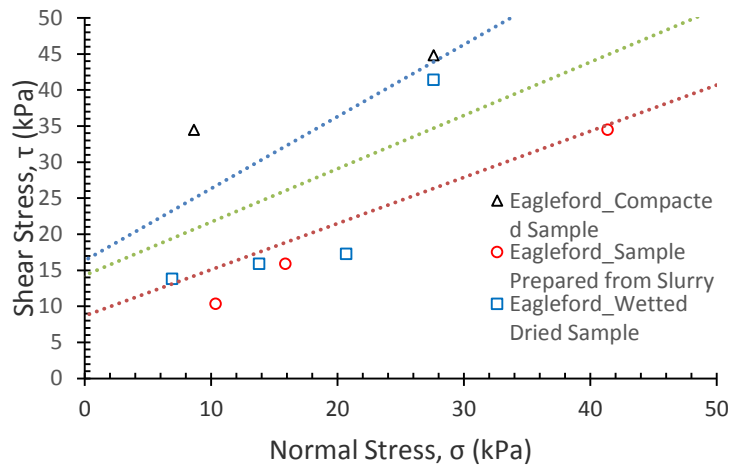


Figure 2-11 Comparison of Wet-Dry Sample Strength with Fully Softened Condition (Wright, 2007)

Though experimental results provide some cohesion at fully softened stage but it is not true for the field condition. These results indicated that, curve failure envelope is required for

shallow slope failure analysis instead of a linear mohr coulomb envelope which provide a constant value of friction angle.

2.4.4.3 Impact on wet-dry cycle on other properties of expansive clay

Zubaydi (2011) conducted some research work with high plastic clay to determine the factors such as number of wetting and drying cycles, loads and soil composition (soil type) affecting swelling/shrinkage, collapsing behavior as well as cracking of compacted soils. Summary of the conclusion of his research is listed below.

- Wetting and drying cycles increases the collapse tendency for clayey soils, while reduces collapse tendency for silty or sandy soils.
- Wetting and drying cycles reduces the degree of expansiveness of clayey soils.
- Cracks area and number of segments amongst cracks increased as the wetting and drying increased

Impact of wet-dry cycle on swelling characteristics are shown in Figure 2-12, indicating a decrease of swelling potential with the increasing number of wet-dry cycle. Though most of the change in swelling potential was observed after 1st cycle but the trend of swell/collapse graphs were the same under each cycle.

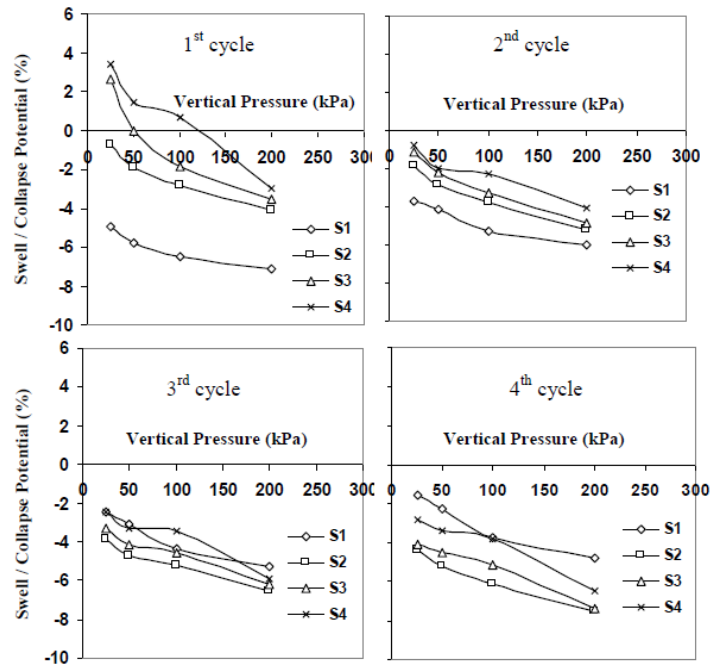


Figure 2-12 Swell Collapse behavior of sample under wet-dry cycle (Zubaydi ,2011)

2.5 Fully Softened Shear Strength

Seasonal variation of rainfall and temperature has an impact on the strength loss of expansive clay over time. A number of researchers are working in this field to understand the fully softened shear strength. Bernardo A. Castellanos (2014), reviewed almost all the previous literature related to the fully softened shear strength. The term “fully softened state of strength” was introduced by Skempton (1970), who considered the fully softened shear strength as a practical approximation of the critical state shear strength.

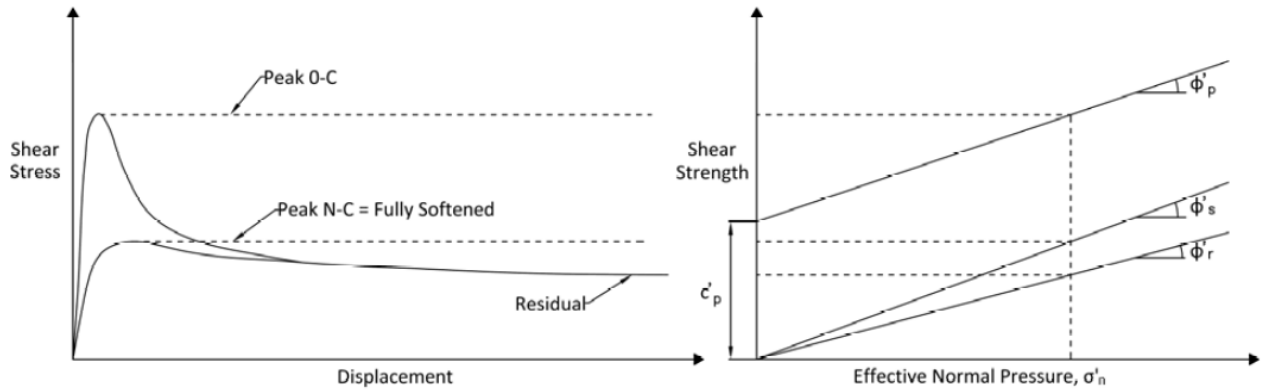


Figure 2-13 Shear characteristics of clays (proposed by Skempton, 1970 and redrawn by Castellanos, 2014)

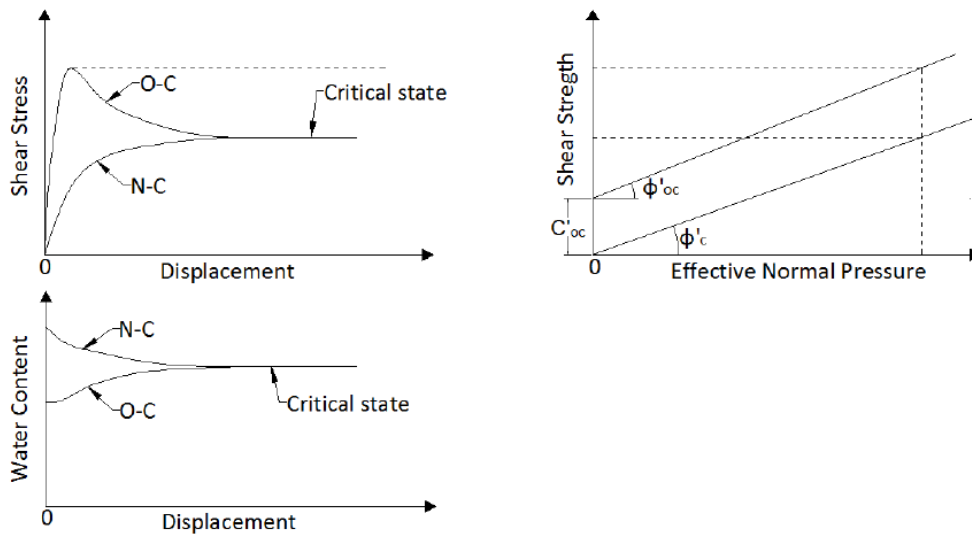


Figure 2-14 Idealized Clay Behavior (proposed by Skempton, 1970 and redrawn by Castellanos, 2014)

According to Figure 2-13 and 2-14, there is a reduction of shear strength after the peak values for the overconsolidated soil. Water content vs displacement curve for

overconsolidated clay (Figure 2-14) shows that, water content increases with displacement which might lead to the decrease of shear strength. Skempton stated that the shear strength in first time slides in London Clay approaches the fully softened shear strength and would normally not be less than that shear strength. Castellanos (2014), represented the chart as shown in Figure 2-15, showing that most probable depth of sliding for the slope constructed with clay should be less than or equal to 5 ft and none of them was recorded beyond 15 ft depth.

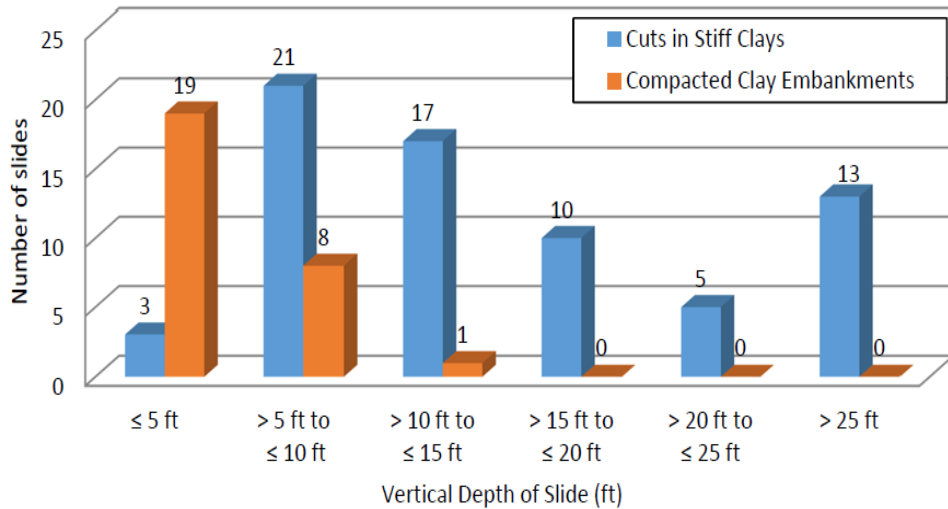


Figure 2-15 Depth of failure of slope constructed with clay. (Castellanos, 2014)

2.5.1 Characteristics of Slope Failure in Texas

Abrams and Wright (1972) reported that, though the design practice of the Texas Highway Department appears in many instances to be satisfactory, but there have been a number of slope failures. According to their study, when these slides develop, the head of the slide mass drops, leaving a 4 to 12 foot scarp, while the toe of the slide bulges and flows down or off the face of the slope, as illustrated by the typical cross section in Figure

2-16. Due to unfavorable geologic and hydrologic condition, majority of the slides have occurred in five Texas Highway Department Districts: Fort Worth, Waco, Austin, San Antoni, and Dallas.

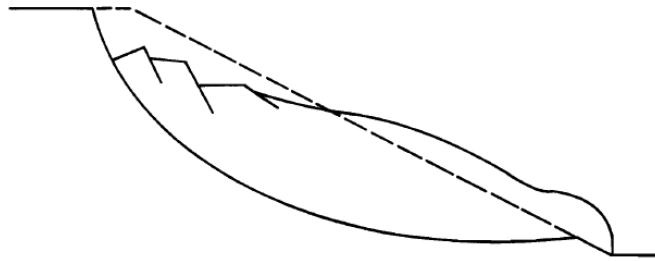


Figure 2-16 Typical failure which occurs in Texas highway cut and embankment slopes
(Abrams and Wright ,1972)

2.5.2 Geological Condition of Texas

In the Fort Worth and Dallas Districts, the Mineral Wells, Eagle Ford, Taylor marl, Denton, and Kiamichi formations are some of the primary geologic formations in which landslides have occurred (Abrams and Wright, 1972). Many of the clays involved in these failures are moderately to highly plastic and some, such as the Eagle Ford, are highly expansive. Plasticity indexes ranging from 35 to 50 have been measured in a number of slides. Frequency of expansive clay in Texas is shown in Figure 2-17, where Dallas area is shown under red zone, indicating a very high expansive clay zone.

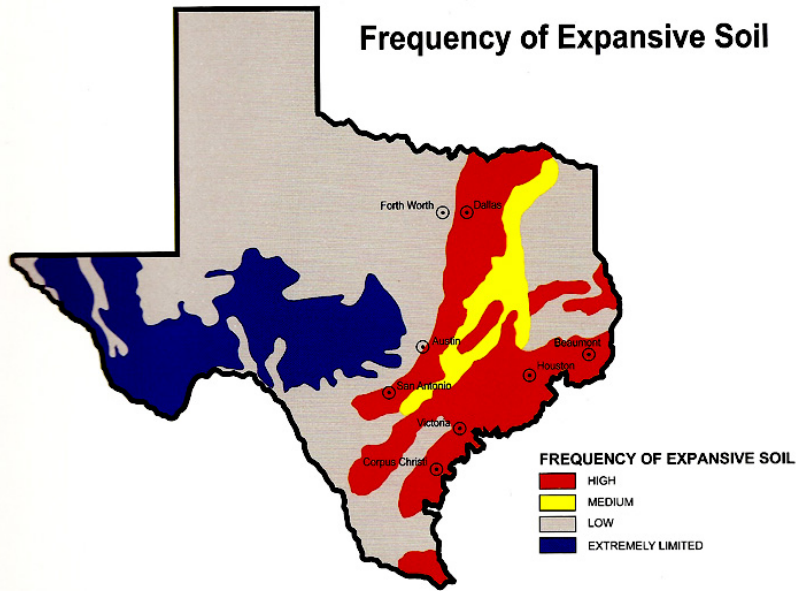


Figure 2-17 Expansive clay map of Texas

(Source: <https://firebossrealtiaroundtown.files.wordpress.com/2014/07/expansive-soil-map.jpg>)

2.5.3 Impact of Climate on Slope Failure

A heavy rainfall after a long summer may increase the chance of shallow slope failure. During a prolonged summer surficial cracks developed and provide preferential path for the rain water to infiltrate into the soil. With the increase of pore pressure, effective soil strength reduces and initiate the first time sliding. A highway slope constructed on US 287, near Midlothian, Texas was constructed with high plasticity clay during 2003-2004. After the construction of the embankment, it went through several wetting and drying period (as shown in Figure 2-18), before the crack at the crest of the slope was observed during 2010 (see Figure 2-19).

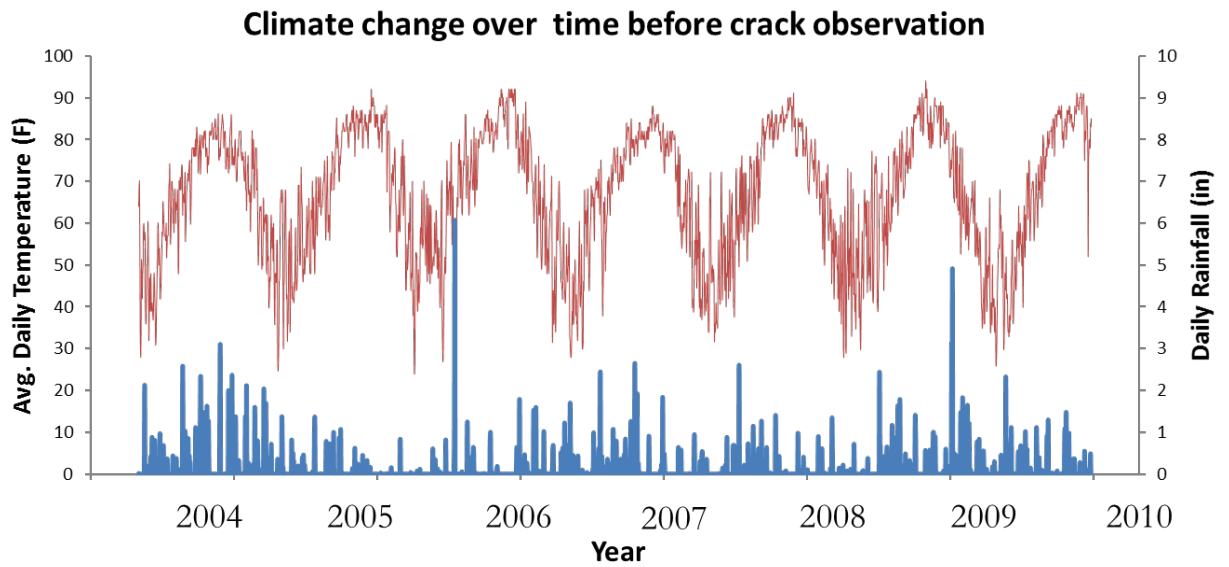


Figure 2-18 Climatic change over time (US 287, Midlothian, Texas)



Figure 2-19 Cracks observed at the crest of the slope at US 287, Midlothian (Sadik, 2013)

2.6 Measurement of Fully Softened Shear Strength

Sample preparation techniques has a remarkable impact on the peak strength value as well as the type of stress-strain curve. It is possible to measure the fully softened

shear strength by direct shear, triaxial, and ring shear tests. Direct shear and triaxial tests are the most common techniques to measure the fully softened shear strength (Bishop et al. 1965; Skempton 1977; Stark and Eid 1997; Stark et al. 2005; Wright et al. 2007). Ring shear device has also been used for this purpose (Stark and Eid 1997; Stark et al. 2005) and standardized procedures have been developed for fully softened ring shear testing (ASTM D7608). VandenBerge et al. (2013), compare the advantages and disadvantages of different shear test apparatus and listed in Table 1.

Table 2-1 Advantages and Disadvantages of apparatus used to measure FSS
(VanderBerg et al., 2013)

	Direct Shear	Ring Shear	Triaxial
Advantages	<ul style="list-style-type: none"> Common Most available Easier to perform Easier to interpret data 	<ul style="list-style-type: none"> ASTM standard available Short consolidation time Small amount of soil needed 	<ul style="list-style-type: none"> Common
Disadvantages	<ul style="list-style-type: none"> One and two weeks required per point No current standard Soil can extrude from the top Top cap can tilt Stress concentrations 	<ul style="list-style-type: none"> Difficult to run tests slow enough for fat clay Sample become thin after consolidation Expensive 	<ul style="list-style-type: none"> Much time required Soft soils are difficult to form into test specimens Difficult to conduct tests at low stresses

Though fully softened sample preparation and testing guideline is only available for ring shear test but there are some disadvantages of using it. Ring shear test is suitable for getting the residual strength but it is not much reliable for fully softened strength. Ring shear test is only suitable for remolded sample but test with different wet-dry cycle is not possible with this apparatus.

2.7 Empirical Correlation to Predict FSSS

Clay-size fraction (CF) and plasticity index are the most common parameters to develop empirical correlations for drained residual and fully softened shear strengths, Skempton (1964), and Mitchell (1993). Skempton observed that, with the increase of clay fraction friction angle of the soil decreases based on the experimental results obtained from different soil (see Figure 2-20).

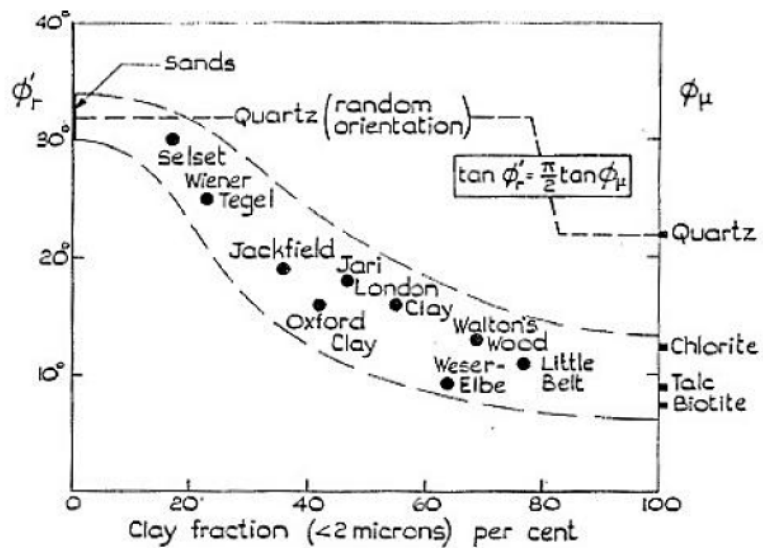


Figure 2-20 Relationship between the clay-size fraction and residual friction angle

(Skempton 1964)

An empirical correlation incorporating effective normal stress, LL, and CF, as suggested by Stark and Eid (1994 and 1997) and Stark et al. (2005), provides a good estimate of the friction angles, which was verified by the back analysis of landslide case histories. Stark and Hussain (2013), updated the correlation developed by Stark et al. (2005) and provide refined equations for three clay fraction groups. They developed a set of three equations (Equation 2.4.1 to 2.4.3) for the empirical correlation for drained fully softened secant friction angles of CF Group No. 1 and for LL values ranging from 30% to less than 80% (30%#LL,80%). It is observed that, soil with same liquid limit and clay fraction will have lower value of friction angle at higher level of normal stress, which indicates the dependency of fully softened strength with normal stress.

$$(\phi'f_s)_{\sigma'n=50 \text{ kPa}} = 34.85 - 0.0709(LL) + 2.35 \times 10^{-4}(LL)^2 \dots\dots\dots (2.4.1)$$

$$(\phi'f_s)_{\sigma'n=100 \text{ kPa}} = 34.39 - 0.0863(LL) + 2.66 \times 10^{-4}(LL)^2 \dots\dots\dots (2.4.2)$$

$$(\phi'f_s)_{\sigma'n=400 \text{ kPa}} = 34.76 - 0.13(LL) + 4.71 \times 10^{-4}(LL)^2 \dots\dots\dots(2.4.3)$$

A set of three equations was also developed for CF Group No. 2 (Clay fraction lies in between 21% to 45%) and LL values ranging from 30% to 130% (30%#LL#130%), and is shown as Eqs. (2.5.1)–(2.5.3).

$$(\phi'f_s)_{\sigma'n=50 \text{ kPa}} = 36.18 - 0.1143 (LL) + 2.354 \times 10^{-4}(LL)^2 \dots\dots\dots (2.5.1)$$

$$(\phi'f_s)_{\sigma'n=100 \text{ kPa}} = 33.11 - 0.107(LL) + 2.2 \times 10^{-4}(LL)^2 \dots\dots\dots (2.5.2)$$

$$(\phi'f_s)_{\sigma'n=400 \text{ kPa}} = 30.7 - 0.1263(LL) + 3.442 \times 10^{-4}(LL)^2 \dots\dots\dots(2.5.3)$$

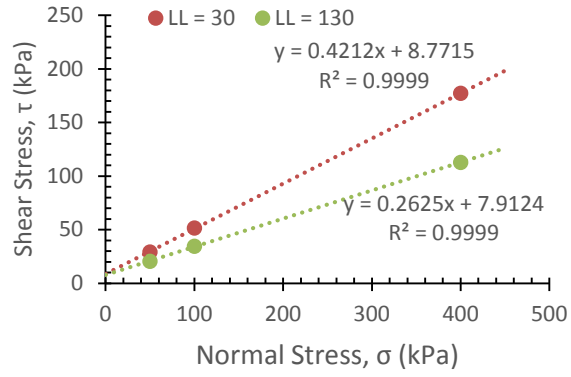
Second degree polynomial function was used to correlate the fully softened friction angle for clay fraction less than 45% but for the soil having clay fraction more than 50% third degree polynomial was used where the LL values ranging from 30% to 300% (30%#LL#300%) and is given as Eqs. (2.6.1)–(2.6.3).

$$(\phi'f_s)_{\sigma'n=50 \text{ kPa}} = 33.37 - 0.11 (LL) + 2.344 \times 10^{-4}(LL)^2 - 2.96 \times 10^{-7}(LL)^3 \dots\dots\dots (2.6.1)$$

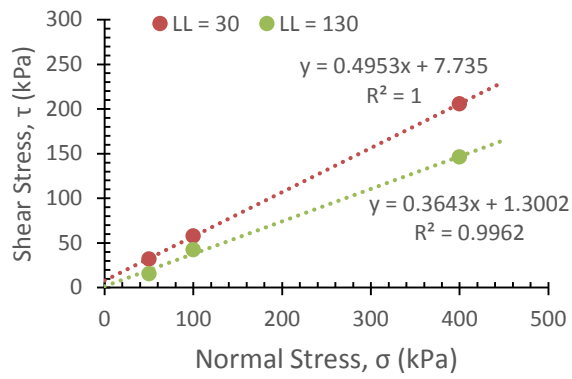
$$(\phi'f_s)_{\sigma'n=100 \text{ kPa}} = 31.17 - 0.142 (LL) + 4.678 \times 10^{-4}(LL)^2 - 6.762 \times 10^{-7}(LL)^3 \dots\dots\dots (2.6.2)$$

$$(\phi'f_s)_{\sigma'n=400 \text{ kPa}} = 28.0 - 0.1533 (LL) + 5.64 \times 10^{-4}(LL)^2 - 8.414 \times 10^{-7}(LL)^3 \dots\dots\dots (2.6.3)$$

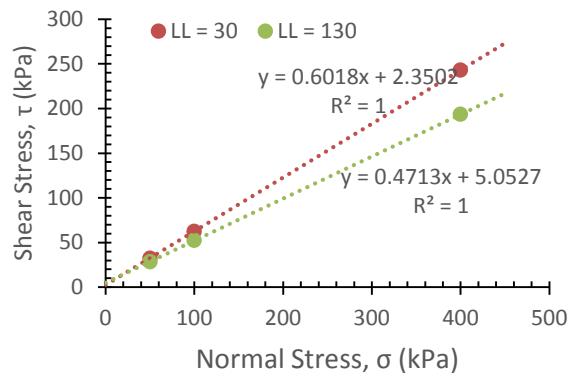
For shallow slope stability analysis, fully softened friction angle at normal stress of 50 kPa may be used but use of cohesion is not recommended. It is possible to calculate the shear strength under each normal stress level and form a failure envelope. Linear failure envelope was constructed for a given set of soils, having a liquid limit of 30 and 130 is shown in Figure 2-21. For each of the cases, linear mohr coulomb envelope was observed with a value of cohesion ranging from 1.3 kPa to 7.9 kPa. But using a value of cohesion for shallow slope stability analysis with a slope which is subjected to drying and wetting will not provide adequate factor of safety.



(a)



(b)



(c)

Figure 2-21 Failure envelope prepared with the empirical correlations (a) for clay fraction less than 20%, (b) for clay fraction 21 to 45% and (c) for clay fraction greater than 50% as provided by Stark and Hussain (2013)

2.8 Effect of sample preparation on fully softened shear strength

It is possible to use undisturbed soil sample in ring shear test but an undisturbed specimen can be used for ring shear testing. Non horizontal shear surface in the ring shear apparatus may be the reason behind inappropriate shear strength. As a result, Stark and Eid (1993) used the ring shear test method following the ASTM D 6467 standard for remolded samples. Stark et al. (2005) concluded that, preparation of a remolded specimen can influence the liquid limit and clay-size fraction measured for the material and thus plotting of the data in Fig. 2-22. Liquid limit value derived from ASTM standard and value obtained after ball-milling are not the same. To reduce the need of commercial laboratory testing with the ball mill, Stark et al. (2005) proposed the following correlation.

$$\frac{\text{ball-milled derived LL}}{\text{ASTM derived LL}} = 0.003 (\text{ASTM derived LL}) + 1.23 \dots\dots\dots (2.7)$$

It is observed that, ASTM derived LL is slightly lower than the liquid limit derived using ball-milled. If the liquid limit of a soil is 100, ball-milled derived LL will be 1.53 times

of ASTM derived LL. If equation 2.5.1 is used to calculate the fully softened friction angle, the ball-milled procedure will yield a shear strength which is 0.59 times of ASTM case.

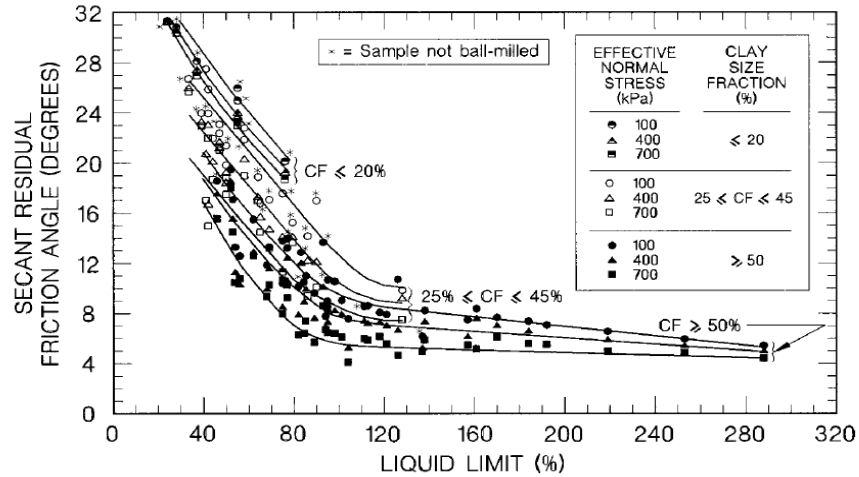


Figure 2-22 Secant residual friction angle relationships with liquid limit, clay-size fraction and effective normal stress

2.9 Difference between residual and fully softened friction angle

For compacted soil sample considerable difference in peak and residual strength is observed. But experimental results (Figure 2-23) obtained by Castellanos (2014), showed that, the difference between peak shear strength and residual strength was very low specially at low level of normal stress. At higher level of normal stress of 6016 psf (288 kPa) a significant peak is observed in strength-deformation graph but at lower level of stresses, below 2016 psf (96.5 kPa), the difference between peak and residual shear strength become insignificant.

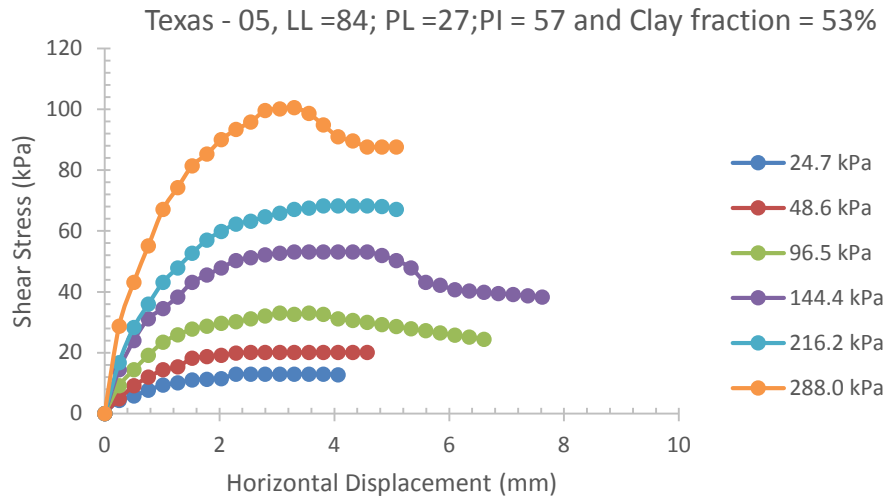


Figure 2-23 Shear test results for Texas soil having LL = 84; PL = 27 and Clay fraction = 53% (Castellanos, 2014)

Numerical difference between the residual (ϕ'_r) and fully softened friction angles (ϕ'_{fs}) for the 36 soils is shown in Figure 2-24, where Stark et al. (2005) reported that, this difference in shear strength is maximized for the soil with liquid limit 80% to 140%. For example, at a liquid limit of 120%, the difference between ϕ'_r and ϕ'_{fs} is approximately 15° and 11° for effective normal stresses of 50 and 400 kPa, respectively.

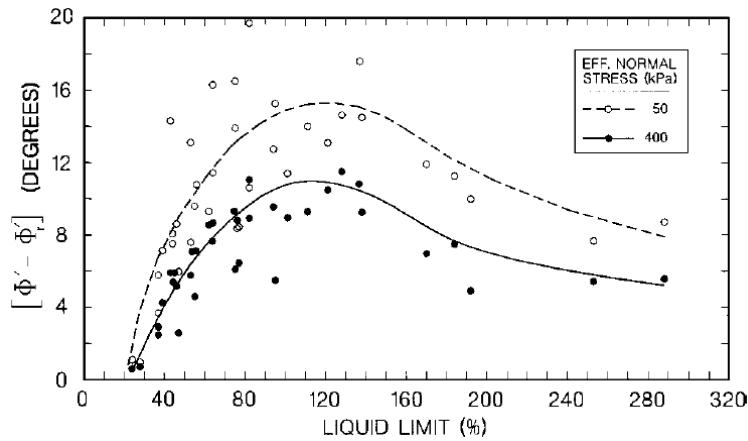


Figure 2-24 Difference between secant fully softened and residual friction angles as function of liquid limit (Stark et al. 2005)

2.10 Use of post peak Shear Strength

At higher level of normal stress, there is a visible peak and residual strength obtained from a direct shear test as shown in Figure 2-23. It is expected that, there will be a non-uniform development of shear stress along the critical slip surface. Use of post peak shear strength for slope stability analysis was proposed by Gregory et al. (2013) where he concluded that, it is required to develop post-peak FSS along the slip surface. He also proposed to use the average shear strength along the failure surface which was somewhere between peak and residual strength.

Table 2-2 Results of slope stability analysis using different percentage of peak strength

(Gregory, 2013)

Slope Ratio	Height (m)	% of Peak shear strength	Maximum depth of slip surface m	r_u	h_w/h
3:1	4.57	100	1.21	0.345	0.76
3:1	4.57	75	1.34	0.281	0.62

Slope Ratio	Height (m)	% of Peak shear strength	Maximum depth of slip surface m	r_u	h_w/h
3:1	4.57	50	1.42	0.195	0.42
3:1	4.57	25	1.60	0.074	0.16
3:1	7.62	100	2.00	0.316	0.70
3:1	7.62	75	2.21	0.244	0.56
3:1	7.62	50	2.42	0.146	0.31
3:1	7.62	25	2.64	0.002	0.00
3:1	10.67	100	2.80	0.296	0.66
3:1	10.67	75	3.08	0.218	0.48
3:1	10.67	50	3.36	0.112	0.25
4:1	4.57	100	1.48	0.500	1.00
4:1	4.57	75	1.64	0.456	0.98
4:1	4.57	50	1.86	0.389	0.83
4:1	4.57	25	1.97	0.294	0.62
4:1	7.62	100	2.57	0.484	1.00
4:1	7.62	75	2.75	0.427	0.92
4:1	7.62	50	3.06	0.350	0.75
4:1	7.62	25	3.39	0.241	0.51
4:1	10.67	100	3.69	0.468	1.00
4:1	10.67	75	3.92	0.407	0.87
4:1	10.67	50	4.34	0.324	0.68
4:1	10.67	25	4.70	0.205	0.43

Gregory varied the pore pressure parameter r_u value for each slope geometry and each strength level, so that resisting force reduces to the driving force. Based on r_u values, h_w/h ratio was calculated using the following equation.

$$r_u = \frac{\gamma_w}{\gamma} \cdot \frac{h_w}{h} \cdot \cos^2\beta \dots\dots\dots (2.8)$$

Where,

γ_w = unit weight of water

γ = unit weight of soil

β = slope angle

Maximum depth of sliding for a 3:1 slope was 3.36 m, having a r_u parameter of 0.112, whereas for a sliding depth of 1.21 m, required r_u parameter was 0.345. For a different slope ratio of 4:1 similar kind of result was observed where, a higher pore pressure distribution parameter was required when the depth of sliding increases.

2.11 FSSS failure envelope

Direct shear test results (Castellanos, 2014) of three soils with different clay fraction and liquid limit is shown in Figure 2-25. For a soil with lower liquid limit (33%) and clay fraction (23%) have a higher value of friction angle and lower value of cohesion but soil with higher liquid limit (83%) and higher clay fraction (63%) provides a higher cohesion and lower friction angle. But experimental results on compacted sample with zero confining stress were conducted by Lade (2010). He performed immerse tests on soil having different clay fraction and liquid limit as shown in Table 2.3. Immerse test was performed by placing the compacted soil cylinder in a 500 ml glass beakers, filled with water up to 1 cm height from the top of the specimen. Results obtained from the air-dried and oven-dried specimen

showed that, at zero confining stress under full saturation there will be no cohesion. If infinite slope stability analysis is used to determine factor of safety one should use, zero cohesion and there is a necessity to use the curved failure envelope instead of linear one.

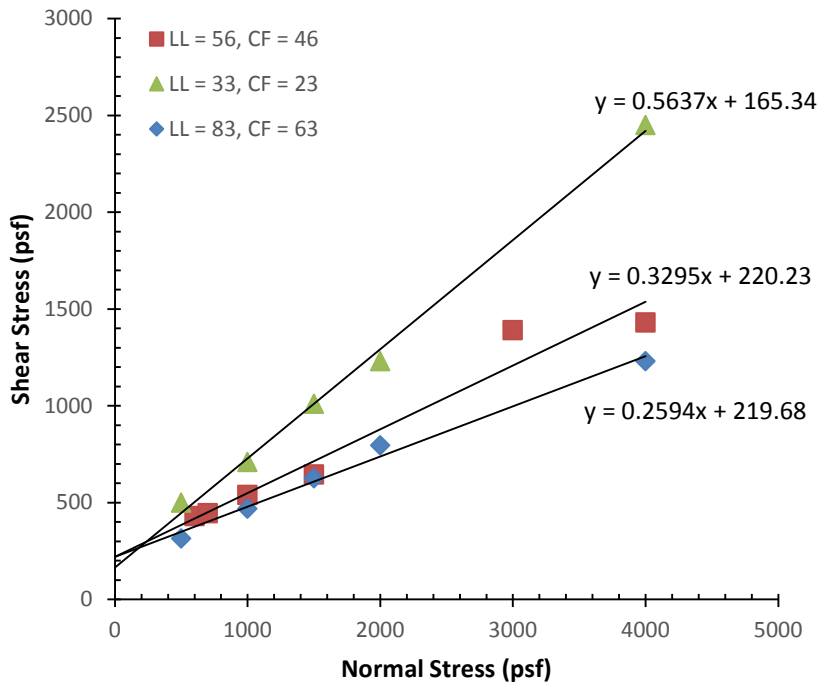


Figure 2-25 Linear failure envelope obtained from direct shear test on fully softened soil with different liquid limit and clay fraction (Castellanos, 2014).

Table 2-3 Immerse test on compacted samples performed by Lade (2010)

Soil No.	Liquid Limit	Plastic Limit	Clay Fraction	Maximum unit weight	Time-to-failure (min)		
					Air-dried specimens	Oven-dried specimens	As-compactd specimens
3	57	29	18	113.5	< 400	25	No failure
6	41	19	12	118.5	26	21	No failure
9	34	15	22	116.5	35	44	No failure
10	30	16	30	127.5	42	29	No failure
11	58	29	26	100.5	16	35	Nearly failed

2.12 Slope stability analysis with curved failure envelope

The linear Mohr - Coulomb failure obtained from the conventional direct shear test results at low level of normal stresses, often provide a higher factor of safety in order of 2 (Lade, 2010). He also reported that, this type of analyses is not appropriate for evaluating of surficial slope stability hence he provide following power function equation (Equation 2.9) which will provide zero cohesion and different friction angle at different level of normal stresses.

$$S = aP_a(\sigma/P_a)^b \dots\dots\dots (2.10)$$

Where,

S = available shear strength

σ = Normal stress

P_a = atmospheric pressure (100 kPa)

a and b are the fitting parameters

Fitting parameters **a** and **b** (Figure 2-26) can be obtained by plotting normalized shear strength vs normalized normal stress curve on a log-log paper. Parameter **a** will be the ration of shear stress and normal stress, corresponding to a value of $\log(\sigma/P_a) = 1$.

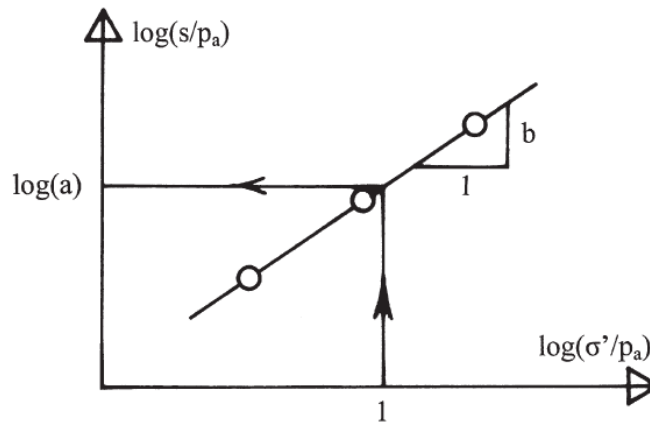


Figure 2-26 Schematic diagram of parameter determination for proposed power function failure criterion.

Factor of safety equation using the fitting parameters is shown in Equation 2.11.

$$F = \frac{s}{\tau} = \frac{a \cdot p_a \cdot (\gamma_w \cdot h \cdot \cos^2 \alpha / p_a)^b}{\gamma_{sat} \cdot h \cdot \cos \alpha \cdot \sin \alpha} \dots\dots\dots (2.11)$$

- S = resisting shear strength
- τ = mobilized shear strength
- γ_{sat} = Saturated unit weight of soil
- γ_w = unit weight of water
- h = depth of sliding
- α = slope angle
- a and b = curve fitting parameters

Chapter 3

Methodology

3.1 Introduction

This chapter presents the sample collection technique, experimental program, soil sample preparation and direct shear testing method. Generally, unless otherwise stated, laboratory testing was performed in accordance with the standards presented by American Society of Testing and Materials (ASTM).

3.2 Sample Collection

Soil samples were collected from two different slope location in Dallas-FortWorth, Texas. (1) The slope located over I35E (North) near Mockingbird lane under TxDOT's Dallas District, designated as "Mockingbird Slope" (Figure 3-1a). (2) The slope located along SH 183 east of the exit ramp from eastbound SH 183 to northbound SH 360 in the northeast corner of Tarrant County of TxDOT's Fort Worth District, designated as "SH 183 Slope" (Figure 3-1b). For both slope soil samples were collected from a depth of 5 to 10 ft. Sample collection from SH 183 site location is shown in Figure 3-1c.



Figure 3-1 Sample Locations

3.3 Experimental Program

Grain size distribution, atterberg limit, specific gravity and other physical properties of the soil samples were determined for the classification of soil. Purpose of the current study is to determine the impact of wet-dry cycle on physical and mechanical properties of expansive clay having different liquid limit. Table 3-1 represents the experimental program to evaluate the change in moisture content, dry density and shear strength properties of soil.

3-1 Experimental Program

Soil Type	Sample ID*	Number of wet-dry cycle	Moisture content	Density	Direct Shear Testing		
					$\sigma = 20$ kPa	$\sigma = 30$ kPa	$\sigma = 40$ kPa
CL	CL_AC	0	6	6	1	1	1
CL	CL_WD_01	1	6	6	1	1	1
CL	CL_WD_03	3	6	6	1	1	1
CL	CL_WD_05	5	6	6	1	1	1
CL	CL_FS	N/A	6	6	1	1	1
CH	CH_AC	0	6	6	1	1	1
CH	CH_WD_01	1	6	6	1	1	1
CH	CH_WD_03	3	6	6	1	1	1
CH	CH_WD_05	5	6	6	1	1	1
CH	CH_FS	N/A	6	6	1	1	1

*First two letter of the Sample ID represents the soil type. Second two letter of the sample ID describe the sample condition prior to testing. Compacted samples are designated by "AC", wetted and dried samples are designated as "WD" and the samples prepared for the fully softened condition is shown as "FS".

3.4 Soil Testing

3.4.1 Sieve Analysis

Sieve analyses were conducted on the collected samples in the laboratory according to ASTM standard D422. Sieve analysis was carried out using 100 gm of air dried samples to determine the particle size distribution. Aggregation of the particles was broken by mortar and rubber covered pestle. The grain size distribution was conducted using a set of US standard sieves (No. 4, 10, 20, 40, 60, 100, 200 and pan). Wet washing was conducted to prevent aggregation of large clumps of fine particles in soil samples retained on sieve No. 200.

3.4.2 Liquid Limit and Plastic Limit

ASTM standard D4318 method - A was adopted to determine the atterberg limit. Soil Samples passing through No. 40 sieve were used in the test. Appropriately, 300 gm soil samples were taken for the determination of liquid limit with Casagrande apparatus. For Plastic limit, soil samples were rolled in the glass plate until they became threads of about 3 mm. When the threads were broken at 3 mm diameter, they were taken in the moisture cans. Samples were dried in the oven and moisture contents were determined for three samples. Average moisture content was reported as the plastic limit of soil.

3.5 Direct Shear Testing

A total of 30 number of direct shear test were conducted under different conditions to evaluate the change in shear strength parameters as shown in Table 3-1. Sample preparation and testing techniques for different conditions are described in the subsequent paragraphs

3.5.1 Compacted Sample

According to ASTM 3080-98 standard, compacted specimen may be prepared by either compacting soil within the shear box mold by kneading or tamping or use different mold of representative size for compaction than placing the sample into the shear box. In this study a separate mold of 2.5-inch diameter with 6 inch height is used for compaction. The soil sample with a moisture content of about 25% was used to compact in three layers with 25 blows each with a 5.5 lb hammer. For the determination of shear strength parameters, at least three identical samples were required. A 6 (six) inch long sample is prepared by compaction was cut into three pieces of equal height of 2 inch. These compacted specimens were kept within a zipped lock bags to prevent the loss of moisture. Just before the testing, soil specimens were trimmed into a height of 1.5 inch to fit in the shear box of 2.5 inch diameter. Figure 3-2 shows the compacted sample preparation technique for the direct shear testing.



Figure 3-2 Preparation of soil samples

3.5.2 Wet-dry Sample

Compacted samples were prepared and transferred into a modified chamber for wetting and drying procedure. An acrylic pipe of 2.55 inch inner diameter and 2.5 inch height was used to keep the sample for wetting and drying. Porous stones were placed at top and bottom of the sample for the easy drainage of water. To prevent the clogging of the porous stone, filter paper was used at top and bottom of the chamber, in between soil and porous stone. A schematic diagram of the wet-dry chamber is shown in Figure 3-3. To prevent the soil loss, filter paper at the bottom of the chamber was sealed as shown in Figure 3-4a. Approximate height of the sample was about 2 inch and the gap between the top of the chamber to the top of the sample was about 0.5 inch, as shown in Figure 3-4b. After placing the sample in the chamber, filter paper was used before putting the porous stone at top of the sample (Figure 3-4c, Figure 3-4d). After placing the compacted sample into the chamber, whole set was immersed under water (Figure 3-5) to saturate the sample for at least 24 hrs.

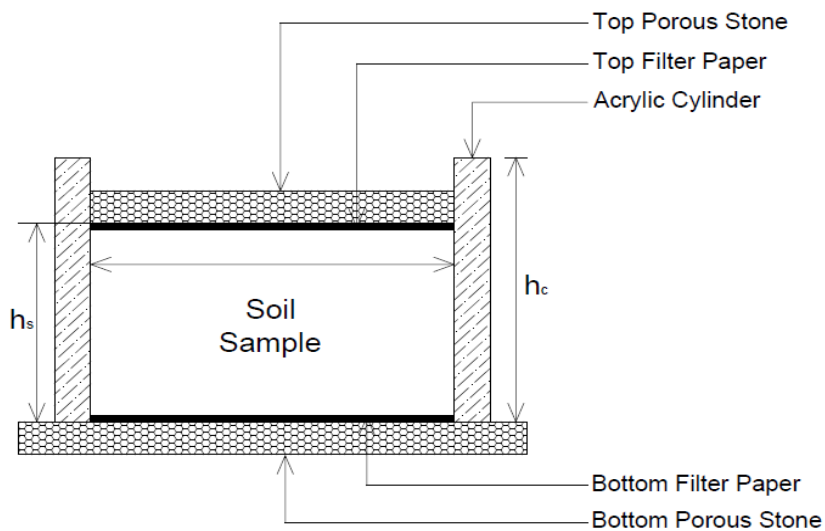


Figure 3-3 Schematic diagram of the wet-dry chamber



Figure 3-4 Placing of soil sample



Figure 3-5 Saturating the sample by adding water

Wetting was followed by a drying period by keeping the chamber in room temperature (70°F) for 24 hrs. After drying sample was set for another wetting period prior to the placing in the shear box. Thus a complete wet-dry cycle consists of wetting, drying and rewetting process. These steps were repeated for further wet-dry cycles.

3-5-3 Fully Softened Sample

Several methods have been adopted by the researchers to prepare the fully softened shear test samples (Wright et al., 2007, Castellanos 2014). For the current study fully softened samples were prepared based on the sample preparation technique proposed by Castellanos, 2014. Fully softened samples were prepared from a soil slurry by adding twice much as water as its liquid limit. Mechanical blender was used for the preparation of soil slurry which was kept in a funnel with filter for the drainage of excess water, as shown in Figure 3-6.

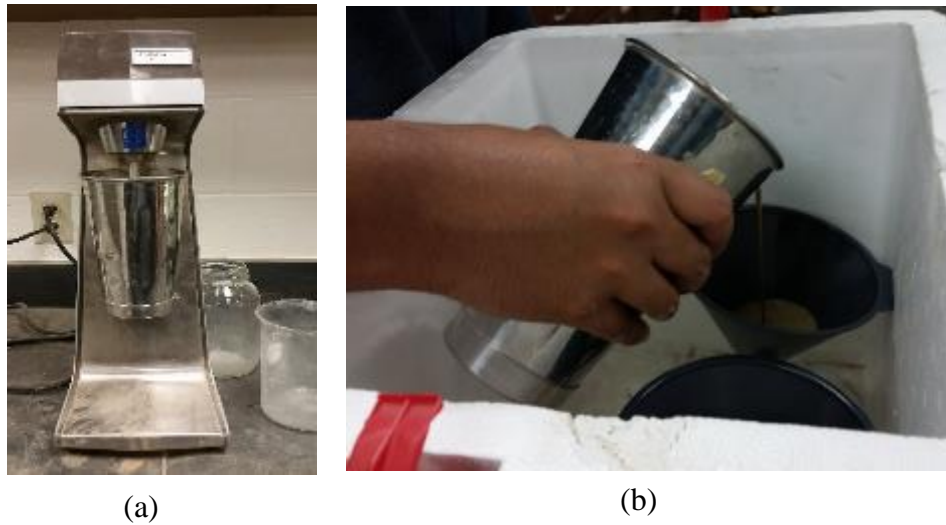


Figure 3-6 Preparation of soil slurry for fully softened shear strength testing

3-6 Direct Shear Test Device

The direct shear test apparatus (HM 2560A, see Figure 3-7) used in this investigation utilizes a pneumatic loading piston for applying the vertical load to the sample. A 2.5 inch diameter shear box is used for testing with maximum possible shear displacement of 0.8 in. It is possible to set the rate of shearing up to 0.001 in/min. The circular test specimens had a diameter of 2.5 inches. The average initial height of the test specimens was around 1.4 inches instead of the normal 1.0 inches. This was done to accommodate the amount of vertical strain that occurs during consolidation of the test specimen

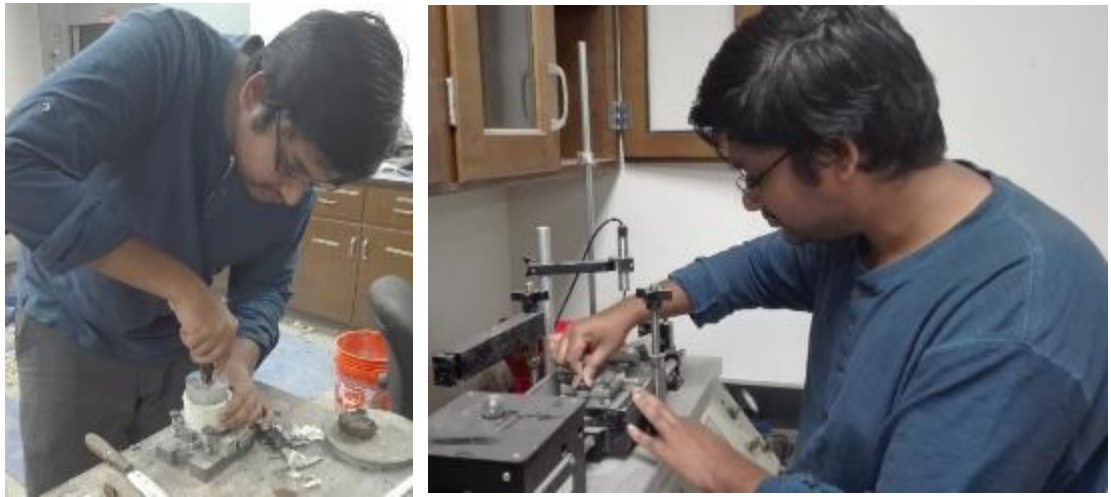


Figure 3-7 Sample placement in direct shear box

3.7 Determination of density, moisture content and void ratio

Soil densities were determined before and after of 1,3 and 5 wet-dry cycle. For the determination of density three identical samples were prepared for each wet-dry cycle. One

of them was used for direct shear testing and two of them were used for the determination of density at initial and final conditions. Bulk density was determined by dividing the weight of the soil with the volume of the soil. After the determination of density, same soil sample was used for the determination of moisture content. Three number of moisture content test were performed to determine the average moisture content.

Void ratios for each cycle were determined for initial and final condition based on soil specific gravity, bulk density and moisture content. Following formula was used to determine the void ratio.

Void ratio,

$$e = \frac{\gamma_w G_s (1 + w)}{\gamma} - 1$$

Here, γ_w = unit weight of water

G_s = specific gravity of soil

W = moisture content

γ = bulk unit weight of soil

Chapter 4

Results and Analysis

4.1 Introduction

Laboratory tests were conducted on collected soil samples from two different locations to determine the impact of wet-dry cycle on the shear strength behavior of clayey soil. The purpose of this chapter is to present the results and analyses of the conducted laboratory tests. Basic Soil properties for the soil collected from two different locations are shown in Table 4.1. Grain size distribution of two soil types is shown in Figure 4-1.

4-1 Soil Properties

Physical Properties	I 35	SH 183
Unified Classification	CH	CL
Liquid Limit	80%	40%
Plastic Limit	18%	10%
Plasticity Index	62%	30%
Percent of Clay	54%	39%
Specific Gravity	2.72	2.75

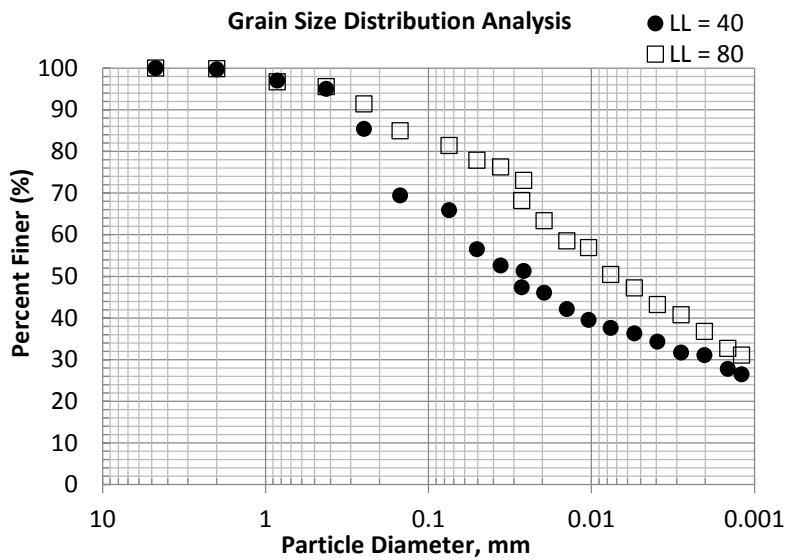


Figure 4-1 Grain Size Distribution Analysis

4.2 Impact of wet dry cycle on basic soil parameters

4.2.1 Impact on moisture content

In this study, low plastic clay (LL = 40) and high plastic clay (LL = 80) were used to determine the change in basic soil properties with wet-dry cycles. For low plastic clay (Figure 4.2a), increase in moisture contents were 51.3%, 63.6.0% and 68.7% for first, third and fifth cycle respectively. Similar trend was observed for the high plastic clay (Figure 4.2b), where the increase in moisture contents were 42.6%, 52.0% and 56.8% for first, third and fifth cycle respectively. Change in moisture content with the increasing number of wet-dry cycle is shown in Figure 4-2.

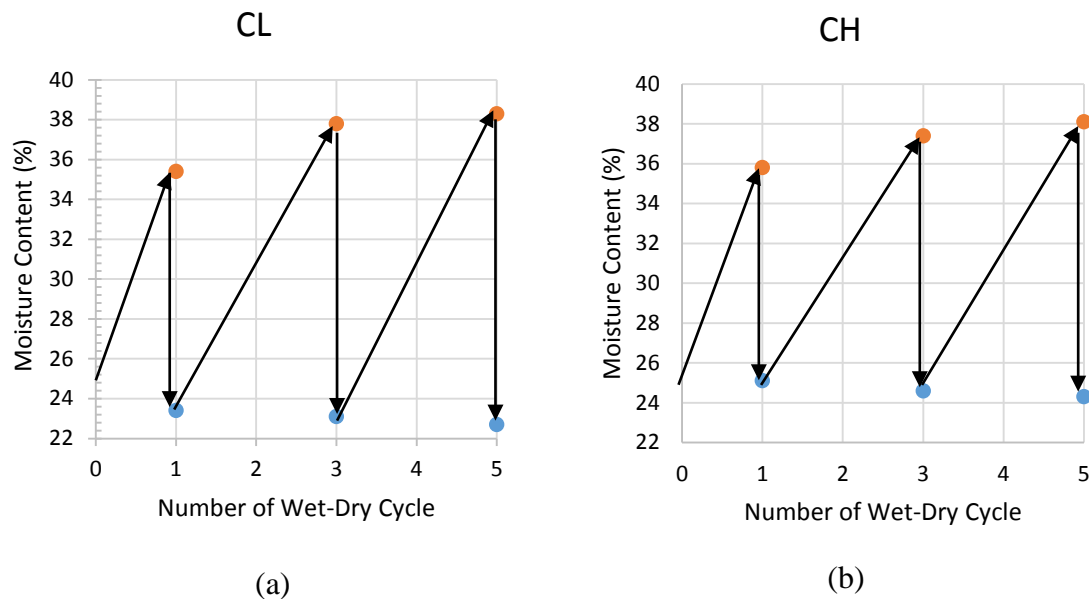


Figure 4-2 Change in moisture content during wetting and drying for a) low plastic clay (LL = 40) and b) high plastic clay (LL = 80)

Change in moisture content for high plastic clay up to fifth wet-dry cycle were compared with the Eagle ford shale (Rogers and Wright, 1986). Figure 4-3 shows that, for Eagle Ford shale, change in moisture content was maximum (57%)

during the third cycle whereas the change in moisture content for the high plastic clay (CH) was maximum (56.8%) after the fifth cycle.

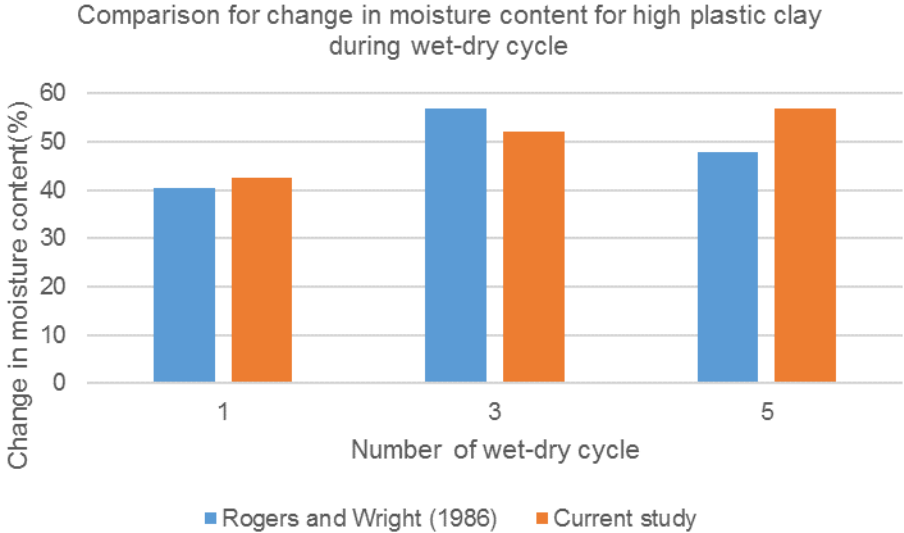


Figure 4-3 Comparison of change in moisture content for high plastic clay during wet-dry cycle

4.2.2 Impact on soil density

Soil density will also change with the wetting and drying procedure as the soil moisture is changing with time. Figure 4-4 represents the change in soil density with number of wet-dry cycle. For low plastic clay (Figure 4-4a), soil density changed from 2 Mg/m³ to 1.94 Mg/m³ and similar trend was observed for the high plastic clay (Figure 4-4b). the decrease in soil density over time may reduce the effective overburden pressure. As the soil density is directly related to its shear strength, there is a possibility of change in shear strength of soil due to wetting and drying.

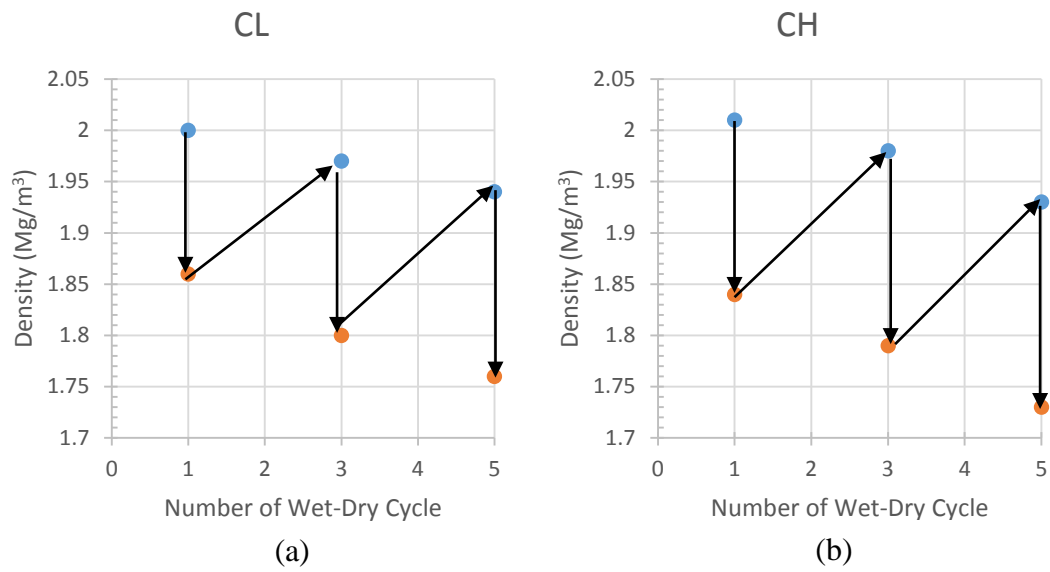


Figure 4-4 Change in soil density during wetting and drying for a) low plastic clay (LL = 40 and b) high plastic clay (LL = 80)

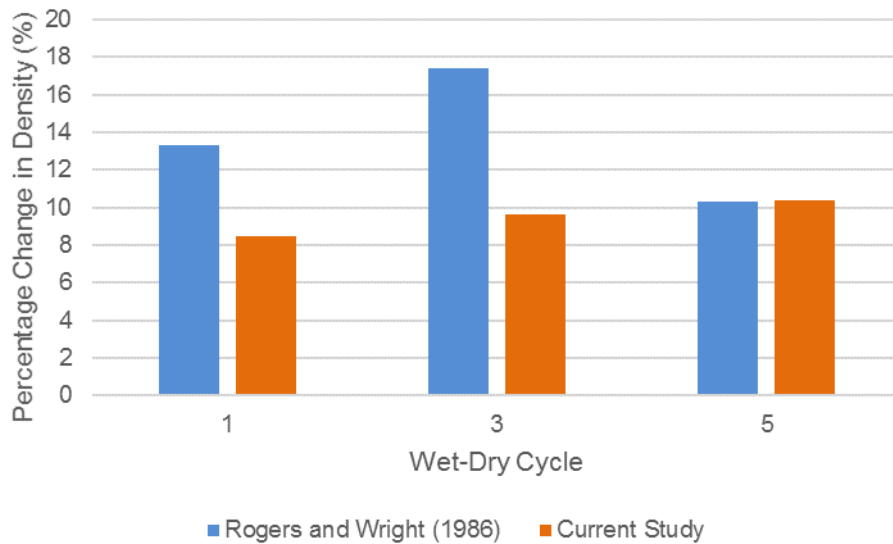


Figure 4-5 Comparison of change in density for high plastic clay during wet-dry cycle

Change in density for high plastic clay up to fifth wet-dry cycle were compared with the Eagle Ford shale (Rogers and Wright, 1986). Figure 4-5 shows that, for Eagle Ford shale, change in moisture content was maximum (17.4%) during the third cycle whereas the change in moisture content for the high plastic clay (CH) was maximum (10.4%) after the fifth cycle. It is observed that, for after the fifth wet-dry cycle, change in moisture content was almost identical.

4.2.3 Impact on void ratio

Experimental results indicate that, void ratio increases with the increase of wet dry cycle as shown in Figure 4-6. For the low plastic clay (Figure 4-6a), change in void ratio for the first, third and fifth cycle were 44.5%, 54.6% and 57.9% respectively. Increase in void ratio with the increasing wet-dry cycle is the indication of volume change over time. Similar trend was observed for the high plastic clay (Figure 4-6b), where the changes in void ratio for the similar number of cycles were 44.7%, 52.0% and 55.0% respectively. It is observed that, for both type of soil, change in void ratio also increases with additional number of cycle. Maximum change of void ratio was observed during the fifth cycle.

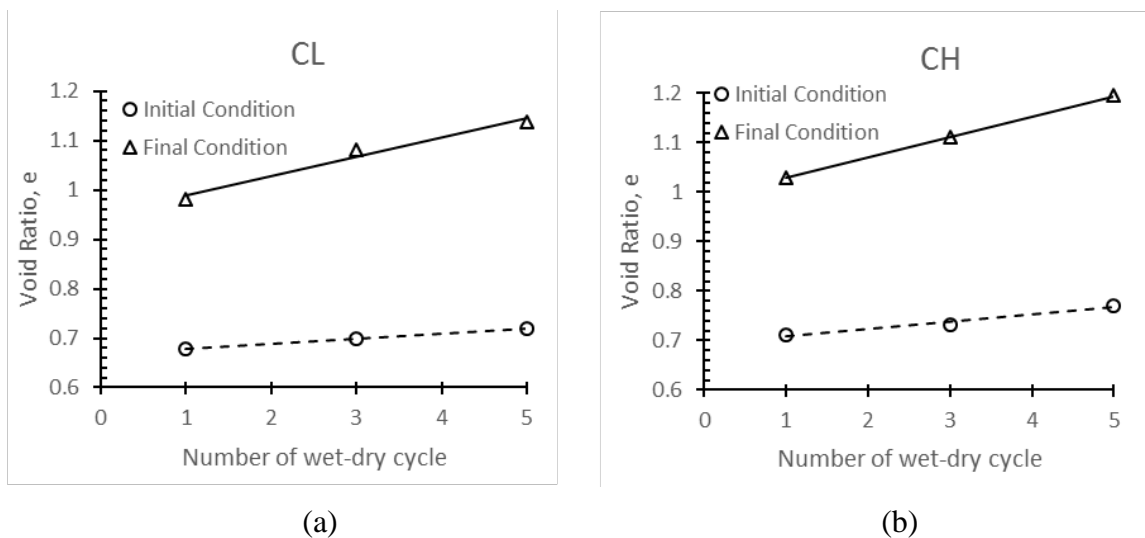


Figure 4-6 Change in void ratio with wet-dry cycle for a) low plastic clay (LL = 40 and b) high plastic clay (LL = 80)

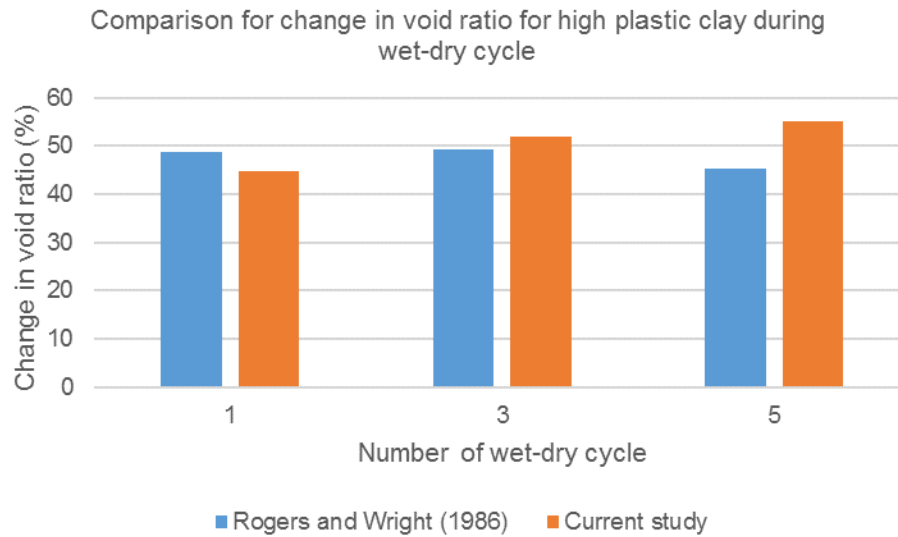


Figure 4-7 Comparison for change in void ratio for high plastic clay during wet-dry cycle

Change in void ratio for high plastic clay up to fifth wet-dry cycle were compared with the Eagle Ford shale (Rogers and Wright, 1986). Figure 4-7 shows that, for Eagle Ford shale, change in void ratio for first, third and fifth cycle were 48.6%, 49.3% and 45.3% respectively. Change in void ratio for the high plastic clay (CH) for the similar number of cycles were 44.7%, 52% and 55% respectively. In case of Eagle Ford shale maximum change of void ratio was observed during the first cycle, whereas maximum change of void ratio was observed after the fifth cycle in case of high plastic clay (CH).

4.3 Stress strain characteristic of soil under different wet-dry conditions

Direct shear test results conducted on compacted sample for both type of soils are shown in Figure 4-8. Figure 4-9, 4-10 and 4-11 represent the direct shear test results conducted after 1st 3rd and 5th wet-dry cycle for both type of clay. Peak shear strength was found to be higher for the soil having lower liquid limit. For both type of soils, it is also observed that, modulus of elasticity is stress dependent. It can be seen that the stress-strain relationships appear to be strain-hardening. The curves show a maximum stress level in each case and after reaching the maximum stress level, there is a slight reduction or tends to reach a steady or equilibrium state in shear stress with increasing horizontal deformation. The results show that the peak shear stress reduce with increasing drying-wetting cycles. The reduction is more pronounced in the 1st cycle and decreases with subsequent cycles and finally reaches to a constant state after 5 cycles.

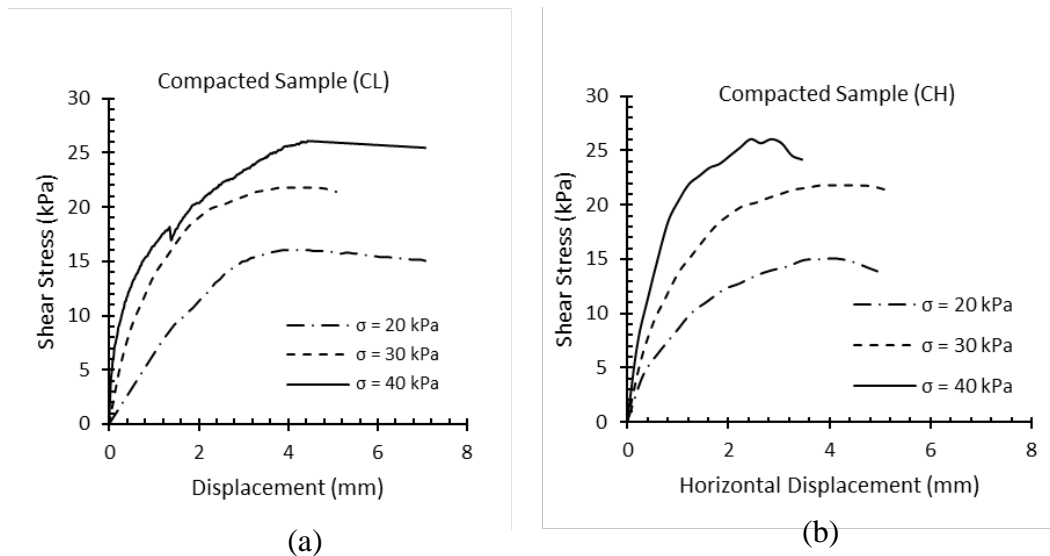


Figure 4-8 Direct Shear Test on Compacted Sample. a) low plastic clay (LL = 40 and b) high plastic clay (LL = 80)

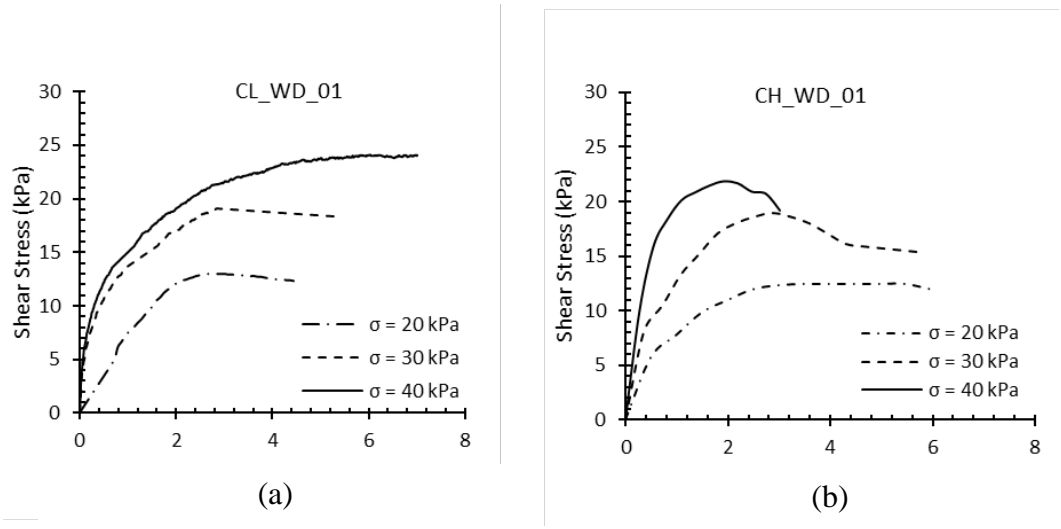


Figure 4-9 Direct Shear Test after 1st Wet-Dry Cycle. a) low plastic clay (LL = 40 and b) high plastic clay (LL =80)

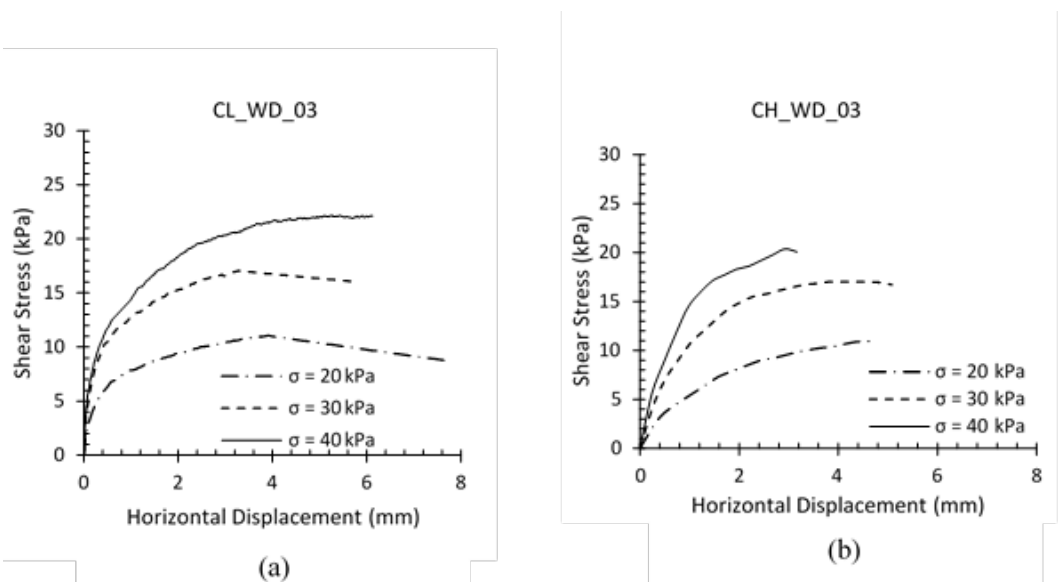


Figure 4-10 Direct Shear Test after 3rd Wet-Dry Cycle. a) low plastic clay (LL = 40 and b) high plastic clay (LL =80)

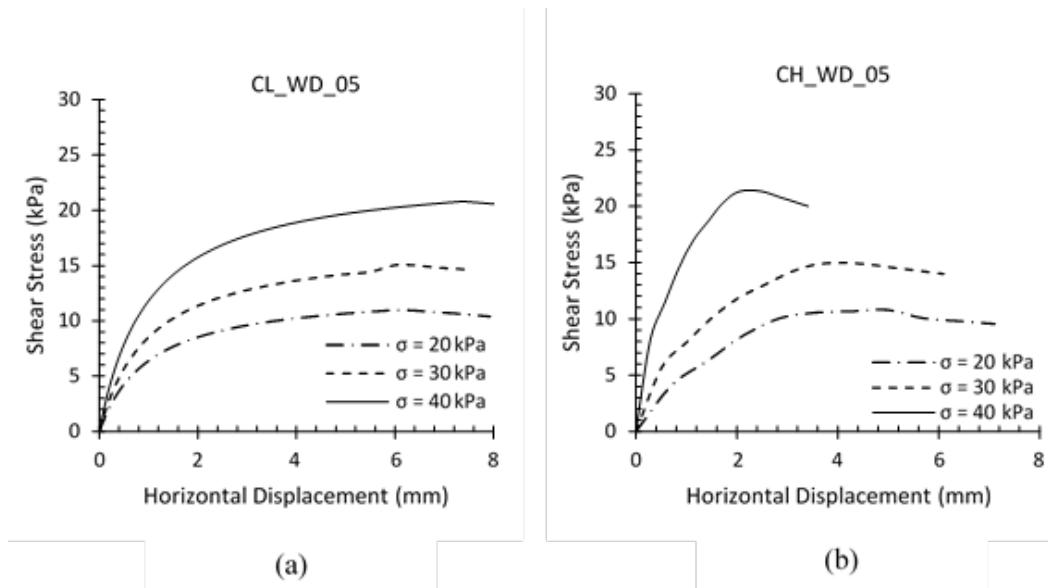


Figure 4-11 Direct Shear Test after 5th Wet-Dry Cycle. a) low plastic clay (LL = 40 and b) high plastic clay (LL =80)

4.4 Attenuation of peak shear stress with wet-dry cycle

The attenuation rate (%) of saturated shear strength with respect to drying-wetting cycles is calculated using following equation

$$\Delta T = \frac{|T_i - T_0|}{T_0} \times 100\%$$

Where, ΔT is the attenuation rate (%), T_0 & T_i are the saturated shear strength of initial and after different

drying-wetting cycles respectively. The variations of saturated shear strength attenuation rate (%) under different net normal stress and drying-wetting cycles are shown in Figure 4-12. For example, in case of high plastic clay (Figure 4.12b) at 30 kpa confining pressure, the attenuation rate is 13.64%, 22.73%, 31.82% for 1, 3 and 5 cycles respectively. The

attenuation rate from cycle 0→1, 1→3, and 3→5 are about 13.64%, 22.73% and 31.82% respectively. It is stated that the attenuation rate is more pronounced in the first cycle and decreases with subsequent cycles. This reduction of shear strength with drying-wetting cycles may be correlated with the change in void ratio and increase of crack and fissure development. Exception of this phenomenon was observed for low plastic soil (Figure 4-12a) there is an abrupt increase in peak shear strength from 1st to 3rd wet-dry cycle at 20 kPa normal stress.

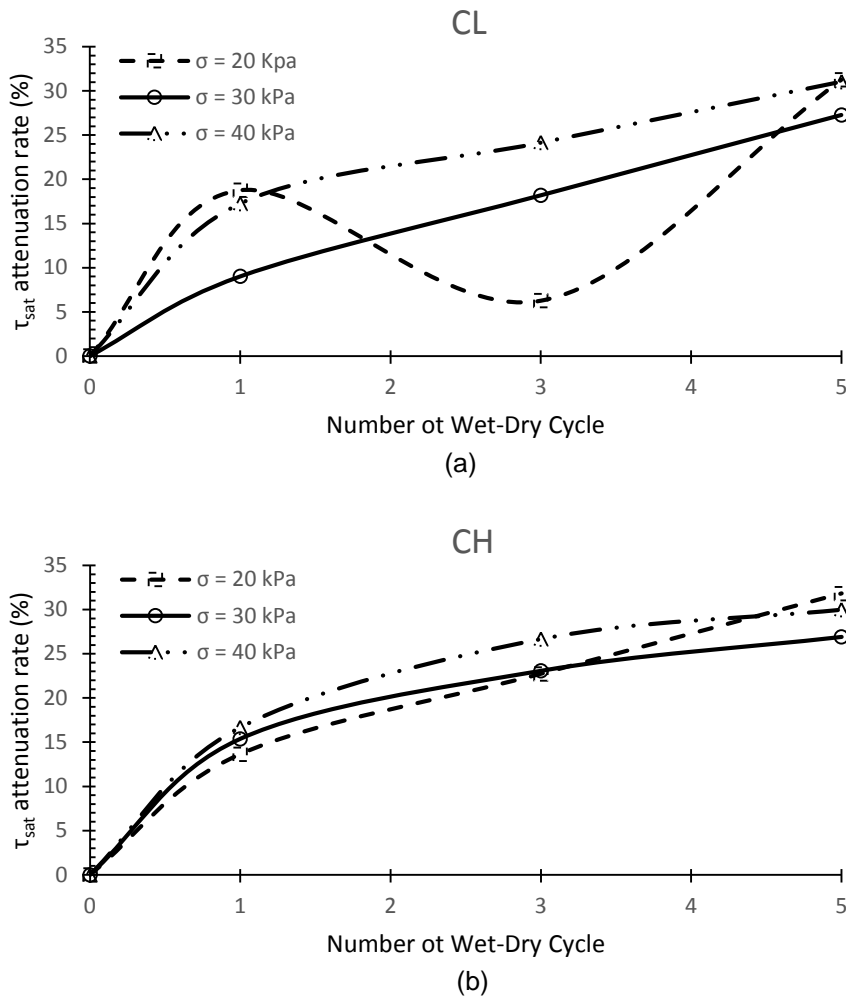


Figure 4-12 Attenuation of saturated peak shear strength with wet-dry cycle. a) low plastic clay (LL = 40 and b) high plastic clay (LL = 80)

4.5 Impact of wet dry cycle on soil cohesion

For the soil with lower liquid limit (40), cohesion obtained for the compacted stage (wet dry cycle number = 0) was 3 kPa, which increases up to 8 kPa after the 3rd wet-dry cycle (Figure 4-13a). Change in void ratio does not have any significant impact on cohesion for this case. On the other hand, soil with higher liquid limit (80), cohesion for the compacted stage was 4.5 kPa which gradually decreased with the increasing number of wet-dry cycle (Figure 4-13b).

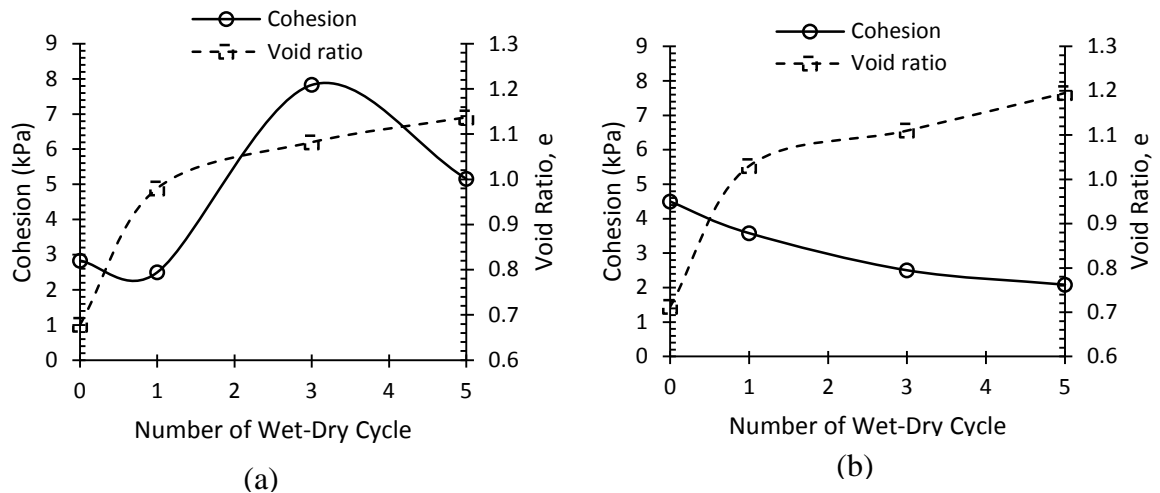


Figure 4-13 Impact of soil wet-dry cycle on soil cohesion. a) low plastic clay (LL = 40 and b) high plastic clay (LL = 80)

4.6 Impact of wet dry cycle on angle of internal friction of soil

Attenuation of peak shear strength with the increasing number of wet-dry cycle, will affect the angle of internal friction of soil. Figure 4-14a represents that, internal friction decreases from 33° to 19° after the fifth wet-dry cycle, for low plastic clay. Decrease in

friction angel was also observed for the high plastic clay, where the angle of internal friction decreases from 29° to 23° after the fifth wet-dry cycle (Figure 4-14b). It is also observed that for low plastic clay, there was a sharp decrease of friction angle up to third cycle and no further change was observed from third to fifth cycle. In case of high plastic clay, there is a gradual decrease in friction angle with the increasing number of wet-dry cycle and total change was 6°, which was much less than the change (14°) observed for the low plastic clay. According to Hossain et al. (2016), wet dry cycle will reduce the cohesion and internal friction for undisturbed residual soil (Figure 4-15). Strength parameters were determined from consolidation drained triaxial test with a higher confining stresses (50 to 300 kPa). Due to a higher overburden pressure consideration, percentage of change in cohesions and friction angles were lower than that observed in this study.

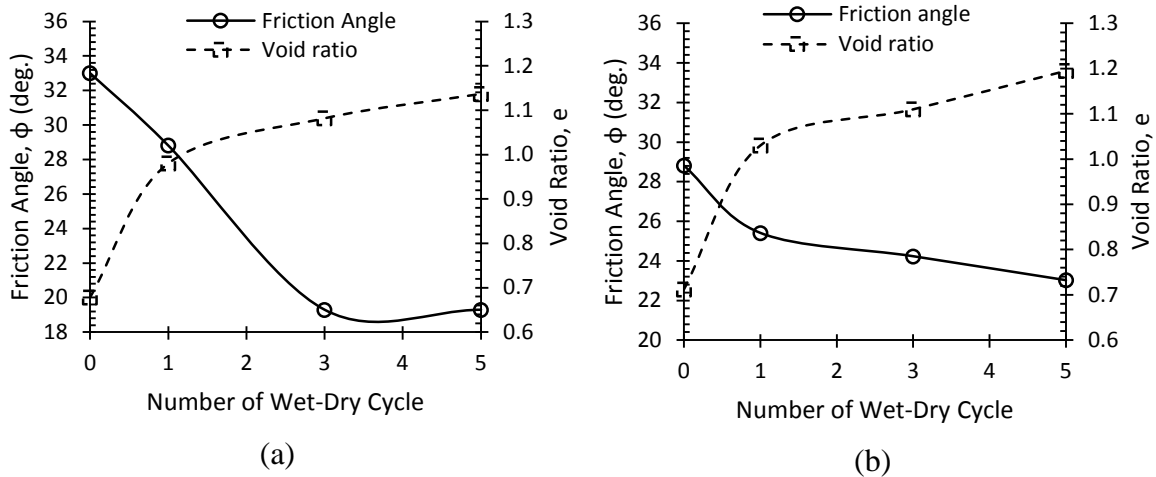


Figure 4-14 Impact of soil wet-dry cycle on internal friction of soil. a) low plastic clay (LL = 40 and b) high plastic clay (LL = 80)

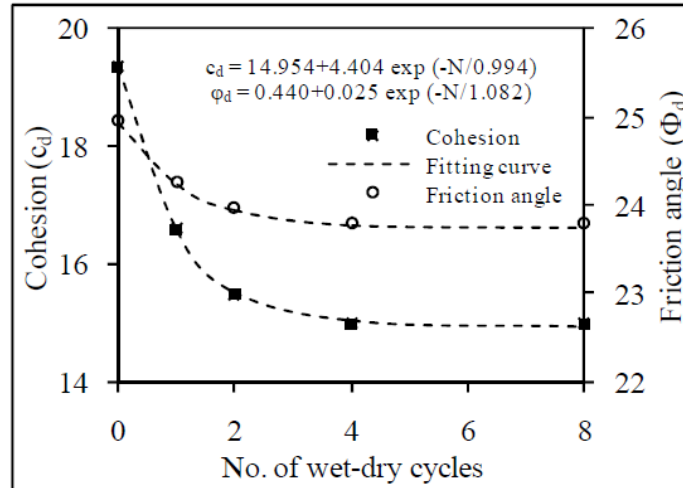


Figure 4-15 Variation of c_d and ϕ_d with respect to drying-wetting cycles (Hossain et al., 2016)

4.7 Impact of wet dry cycle on failure envelop

Results obtained from the direct shear test on wet-dry samples prepared from two types of clay soil of different liquid limit of 40 and 80 are shown in Figure 4-16a and Figure 4.16b respectively. To simulate the shallow slope failure normal stress were kept under 50 kPa (20, 30 and 40 kPa). Though there is a decrease in shear strength with the wet-dry cycle, but it is very difficult to relate the strength with field conditions. Following observation can be made from the results obtained from the wet-dry samples.

- i. Shear strength available at any particular normal stress will decrease with the increased number of wet-dry cycle. For example, at 40 kPa normal stress, peak shear strength of the low plastic clay decreased by 31% after the fifth cycle of wetting and drying. Similarly, peak shear strength for high plastic clay also decreased by 26.9%.

- ii. Shear strength available after 5th wet-dry cycle was found to be similar as fully softened shear strength
- iii. For high plastic clay, the change in friction angle was very small, but the cohesion decreased by 44.44%, whereas the change in friction angle for the low plastic clay was about 9.52°, but an abrupt increase of cohesion was observed after the 3rd cycle of wetting and drying
- iv. It is observed that, for both type of soil, shear strength decreased with wet dry which will have a significant impact on the slope stability analysis.

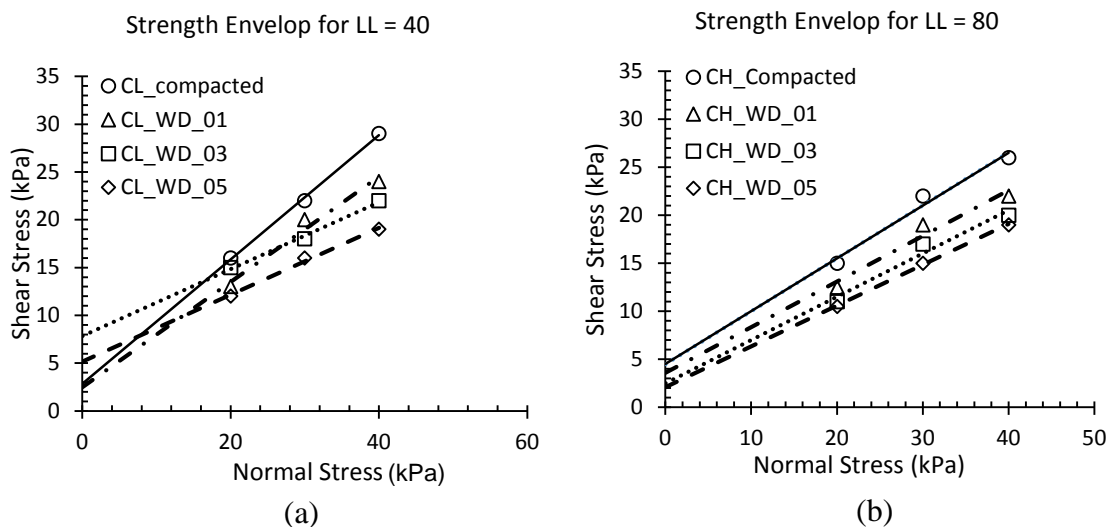


Figure 4-16 Direct shear test results on sample subjected to different wet-dry cycles. (a) Failure envelope for low plastic clay with LL = 40, (b) Failure envelope for high plastic clay with LL = 80

Rogers and Wright (1986) measured the shear strength parameter for Eagle ford shale, under 1,3,9 and 30 number of wet-dry cycle. It is observed that, peak shear strengths under 20, 30 and 40 kPa normal stresses increased by 36.1%, 29.7% and 26.3% respectively in

between first to third cycle (Figure 4-17). Current study shows that, for high plastic clay, under 20, 30 and 40 kPa normal stresses decreased by 17.8%, 16.7% and 16% respectively from the first to third cycle (Figure 4-18). Rogers and Wright (1986) found that, after the 30 cycle of wetting and drying cohesion decreased to zero but the difference between available shear strength from first to 30th cycle under 20, 30 and 40 kPa normal stresses were 3.0%, 8.1% and 10.9% respectively (Figure 4-19). Soil strength varied under repetitive wetting and drying cycle but the strength available after 1st wet-dry cycle was the lowest. In this current study up to 5 cycle of wetting and drying were conducted to observe the change in shear strength at low overburden stress. It is observed that, reduction of strength between first to fifth cycle, under 20, 30 and 40 kPa normal stresses were 27.4%, 26.2% and 25,4% respectively (Figure 4-20).

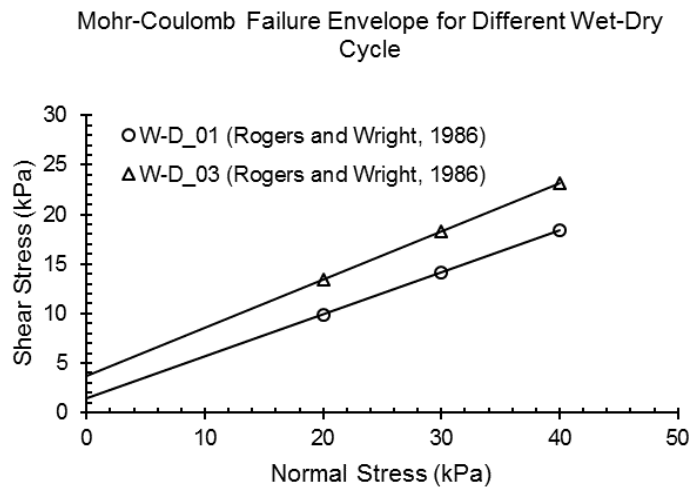


Figure 4-17 Change in shear strength from 1 to 3 cycle (Rogers and Wright, 1986)

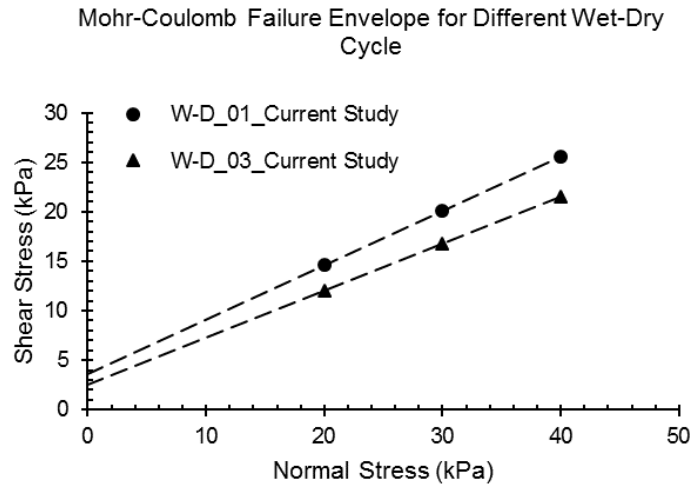


Figure 4-18 Change in shear strength from 1 to 3 cycle (Current Study)

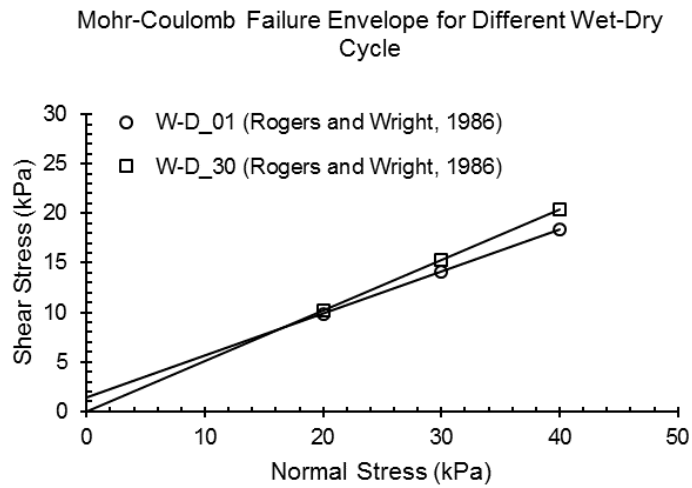


Figure 4-19 Change in shear strength from 1 to 30 cycle (Rogers and Wright, 1986)

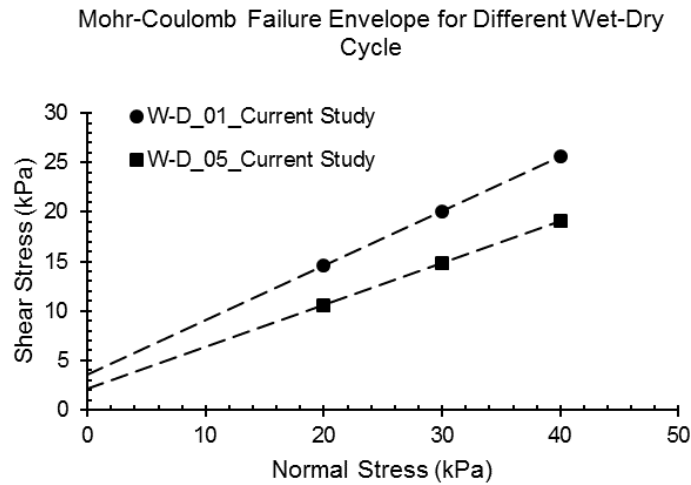


Figure 4-19 Change in shear strength from 1 to 5 cycle (Current Study)

4-8 Determination of fully softened shear strength

Determination of fully softened shear strength at stresses below 50 kPa, is very important for the analysis of shallow slope failure. Strength available during the first time sliding can be reported as the fully softened shear strength (Castellanos, 2014). Repetitive wetting and drying reduces the soil shear strength from compacted stage to the fully softened stage. Fully softened shear strength for two different types of clay, were determined to compare the impact of liquid limit as well as to compare this strength with the strength available after different wet-dry cycle. Fully softened shear test results for clay with liquid limit 40 and 80 are shown in Figure 4-21 and Figure 4-22 respectively. Fully softened friction angle obtained from Wright et al. (2007), was much higher than the results

obtained for low plastic and high plastic clay in this study (Figure 4-23). Using a high overburden pressure might be the reason for getting a higher angle of internal friction.

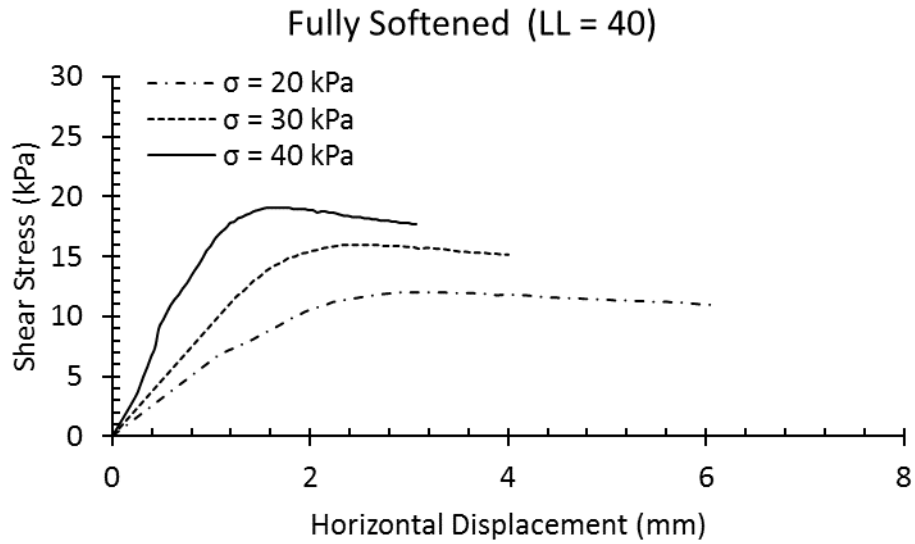


Figure 4-20 Direct shear test for fully softened soil (LL = 40)

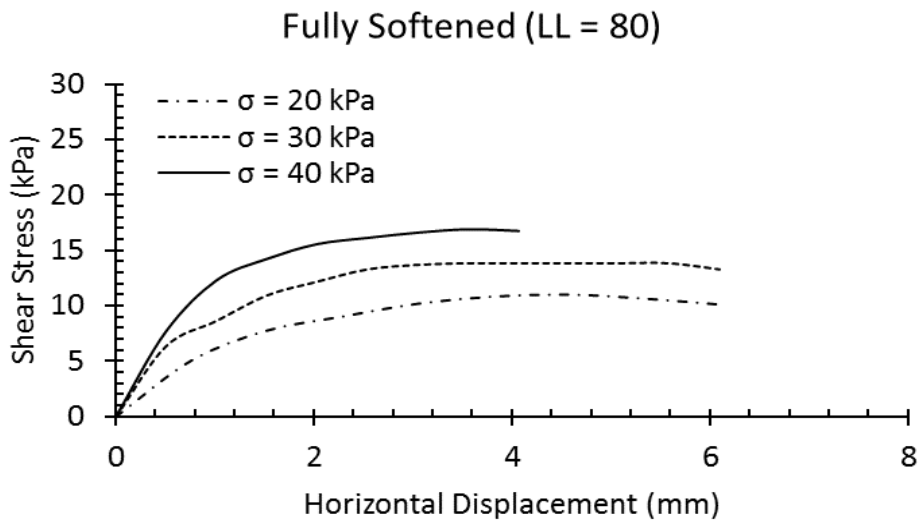


Figure 4-21 Direct shear test for fully softened soil (LL = 80)

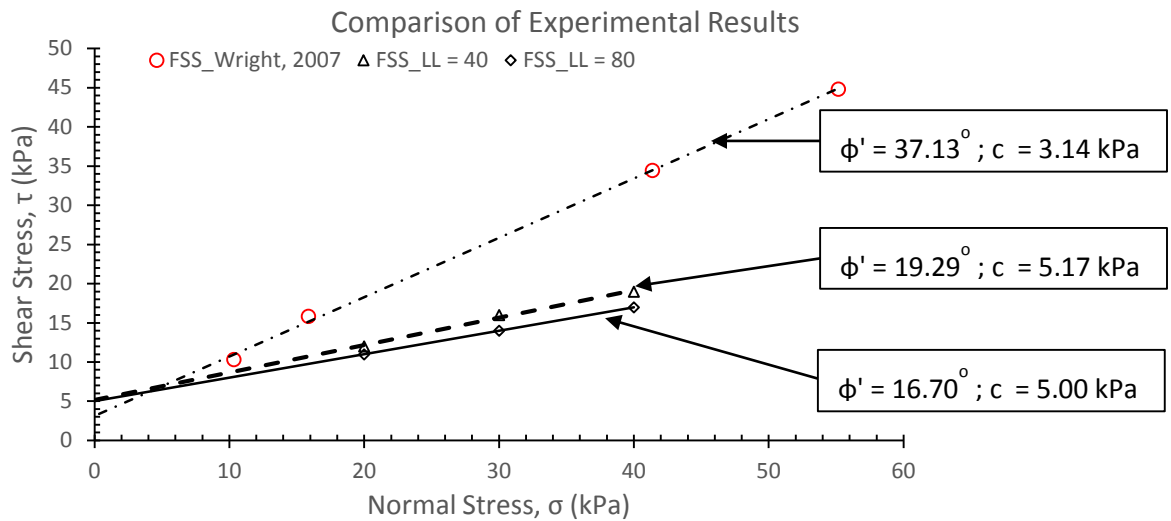


Figure 4-22 Fully softened shear strength comparison for Eagle ford shale and soil sample collected from the DFW area.

Results obtained from this research showed that, fully softened friction angle at very low level of stress might have a very lower value as shown in Figure 4-23. Comparing the experimental results with previous researchers (Wright et al., 2007), following observations are made.

- i. Fully softened friction angle of 37.13° reported by Wright et al. (2007), is not directly applicable for shallow slope failure analysis. Even a zero cohesion value and pore pressure parameter greater than 0.5 with a 1V:2H slope will not fail, with this higher friction angle.
- ii. Based on shallow slope failure investigation in Texas by Gregory (2011), concluded that, to simulate the shallow failure conditions in slopes with ratios

in the range of 3:1 to 4:1 and heights of 15 to 25 feet required an unrealistically high water surfaces (pore pressures).

- iii. Results obtained from current research showed that, fully softened friction angle with soil liquid limit 40 and 80 were 19.29° and 16.7° respectively.
- iv. Even with a low value of friction angle, there exists a cohesion intercept if linear Mohr coulomb failure envelope is used.
- v. Due to wetting and drying cycle, soil strength will decrease up to a certain depth in the slope where the cohesion will be negligible or zero as represented by fully softened condition. Instead of linear Mohr Coulomb envelope, curved envelope is required.

4.9 Comparison of Fully Softened Shear Strength Based on Empirical Correlations

There are some correlations exist between shear strength of soil with liquid limit. Based on the lab test results of soil having a liquid limit range from 30 to 280, Stark et al. provided a total of 9 equations for three different normal stress level to calculate the fully softened friction angle. Based on the empirical correlation failure envelopes for soil with different liquid limit are compared with the current test results. As there is no empirical correlation to find the friction angle at a normal stress below 50 kPa, so failure envelope may be produced by connecting the data point which is fairly a straight line with a zero cohesion intercept. Though the focus of the current study is limited to 50 kPa normal stress, a portion of Figure 4-24a is reproduced (see Figure 4-24b) to give more emphasis on shallow slope failure cases. From 0 to 50 kPa normal stress there is no correlation available, so this portion of the failure envelope is fairly linear. Experimental data showed

that, at lower level of normal stress, failure envelope is curved which means friction angle will change with normal stress.

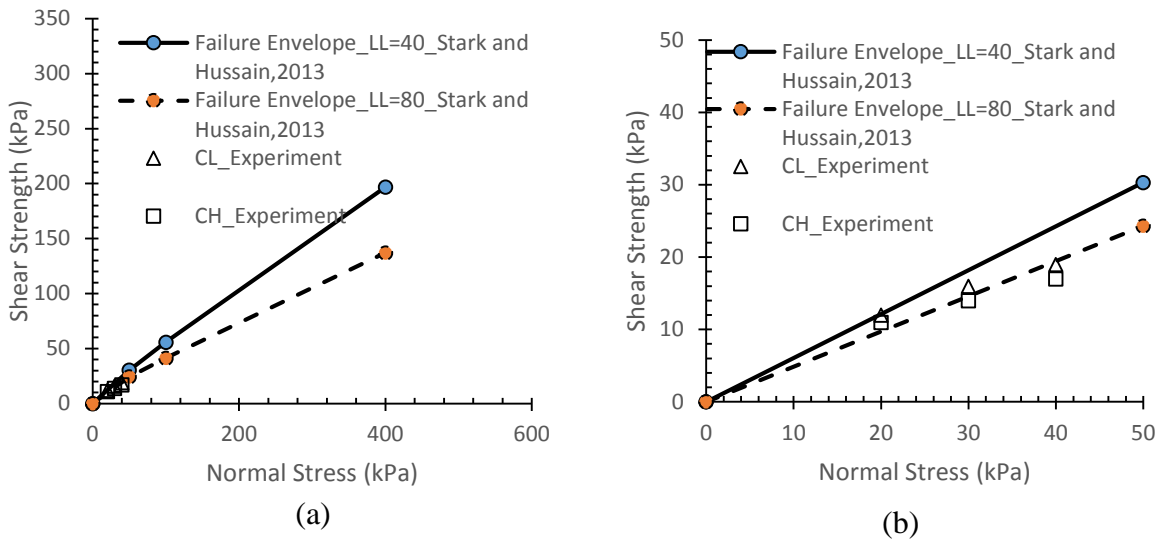


Figure 4-23 Comparison of Experimental Results with Stark and Hussain (2013), Correlation. (a) Failure envelope up to 400 kPa normal stress (b) Failure envelope up to 50 kPa

4.10 Factor of Safety Analysis

Lade (2010), provided the mechanism for shallow slope failure considering an infinite slope with ground water level at the slope surface. It is also assumed that, seepage will occur parallel to the slope surface and weathered layer is underlined by an impermeable layer. Factor of safety was determined for a slope with 3H:1V and considering the saturated unit of soil to be 120 pcf. Factor of safety analysis with different strength parameters obtained from different wetting and drying conditions are shown in Figure 4-24 and Figure 4-25 for soil with liquid limit 40 and 80 respectively. It is evident that for both

type of soils, chances of shallow slope failure increases with the increasing number of wet-dry cycle. After the fifth cycle of wetting and drying depth of failure surface reduced to 3.5 ft for both type of soils.

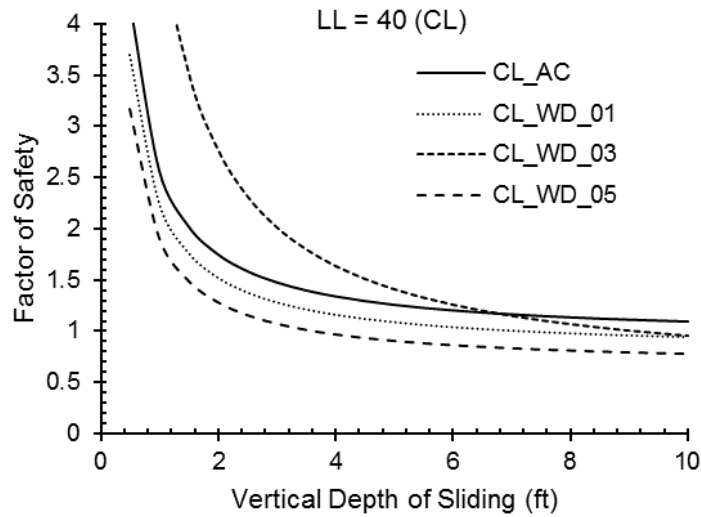


Figure 4-24 Factor of Safety Analysis for CL Soil (LL = 40)

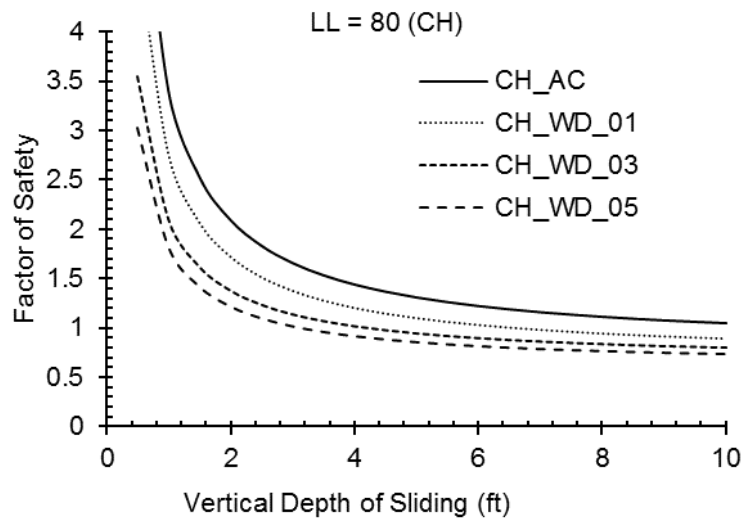


Figure 4-25 Factor of Safety Analysis for CL Soil (LL = 80)

Fully softened shear strengths measured with these soil are also compared with the fully softened shear strength of Eagle Ford Shale (Wright, 2007), obtained from high confining pressure. It is observed that, for the slope with same configuration stated above, will not fail with the strength obtained from high confining stress. For Eagle Ford Shale, the factor of safety up to a depth of 10 ft will be greater than 1.5. (Figure 4.26). On the other hand, shear strength obtained at low overburden stress (< 50 kPa) for liquid limit of 40 and 80 provided the depths of sliding of 5.4 ft and 4.6 ft respectively.

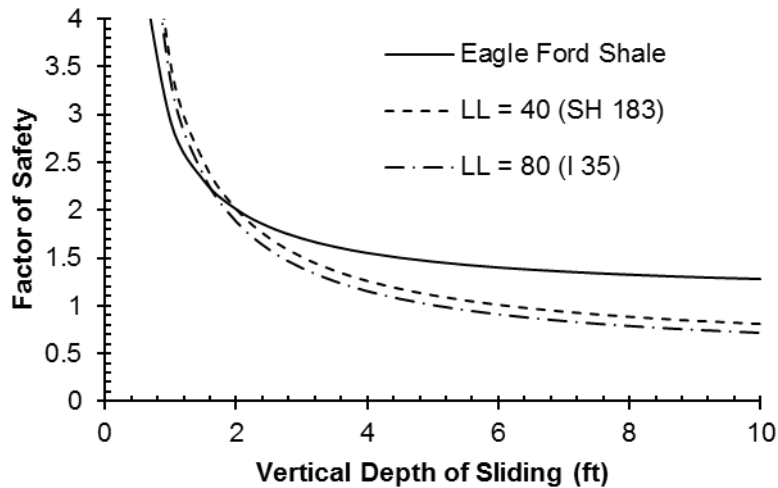


Figure 4-26 Comparison of Factor of Safety based on Fully Softened Strength

Summary of factor of safety analysis to find the critical depth of sliding is also shown in Table 4-2. It is observed that, wetting and drying cycle reduced the shear strength and increase the possibility of shallow slope failure. For both type of clays, no failure was observed at compacted strength and minimum critical depth was found after the fifth cycle. It is also observed that, depths of failure for both type of clay obtained from the shear strength parameters after fifth cycle were lower than the fully softened shear strength.

Table 4-2 Critical Depth of Failure Based on Shallow Slope Mechanism

S.N.	Soil Type	Sample ID	Soil Strength Parameters		Critical Depth of Failure (ft)
			c (kPa)	ϕ	
1.	Low Plastic Clay (LL = 40)	CL_AC	2.83	33.0°	No failure
2.		CL_WD_01	2.50	28.8°	6.8
3.		CL_WD_03	7.83	19.3°	No failure
4.		CL_WD_05	2.17	24.2°	3.5
5.		CL_FS	19.29	5.2°	5.6
6.	High Plastic Clay (LL = 80)	CH_AC	4.50	28.8°	No failure
7.		CH_WD_01	3.58	25.4°	6.5
8.		CH_WD_03	2.50	24.2°	4.4
9.		CH_WD_05	2.08	23.0°	3.2
10.		CH_FS	16.70	5.0°	4.8

Chapter 5

Conclusion and Recommendations

5.1 Summary and Conclusion

Wetting and drying cycle reduces the shear strength of the soil. The reduction of strength over time will also reduce the factor of safety to unity when the first time slide will occur. Historical data from the first time slide of a compacted slope provided that, available shear strength is quite below the compacted strength and comparable with fully softened shear strength. Results obtained from low plastic clay (LL = 40) are shown in Figure 5.1 and Table 5.1. Change in physical and mechanical properties of high plastic clay are shown in Figure 5.2 and Table 5.2 respectively. Following are the observations of this study.

- i. Percentage increase of moisture content was as high as 67% for low plastic clay during the fifth cycle. In case of high plastic clay change in moisture content was about 57% after the fifth cycle.
- ii. Percentage increase in void ratio was more than 50% for both type of soil, after the fifth cycle
- iii. For LL = 40, an increase in cohesion was observed after the fifth wet-dry cycle, though the friction angle decreased from the compacted condition. For LL = 80, cohesion decreased with the increased number of wet-dry cycle.
- iv. Angle of internal friction reduces by 14° and 6° for low plastic and high plastic clay respectively
- v. Shear strength available after 5th wet-dry cycle was found to be lower than the fully softened shear strength.

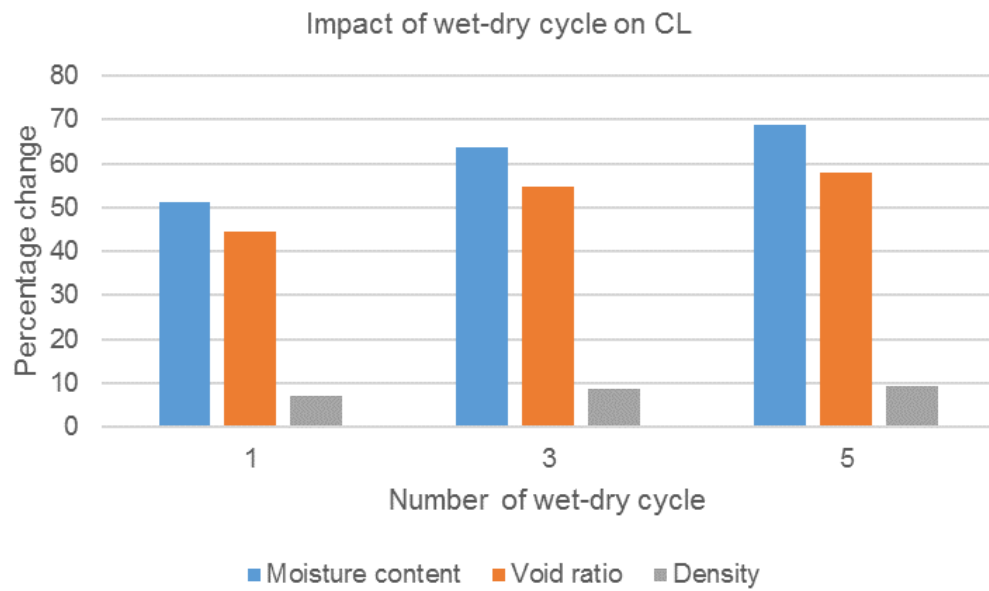


Figure 5-1 Impact of wet dry cycle on physical properties of CL (LL=40) soil

Table 5-1 Impact of wet-dry cycle on the mechanical properties of CL (LL=40) soil

W-D Cycle	c	ϕ
0	2.83	33.00
1	2.50	28.81
3	7.83	19.30
5	5.16	19.20

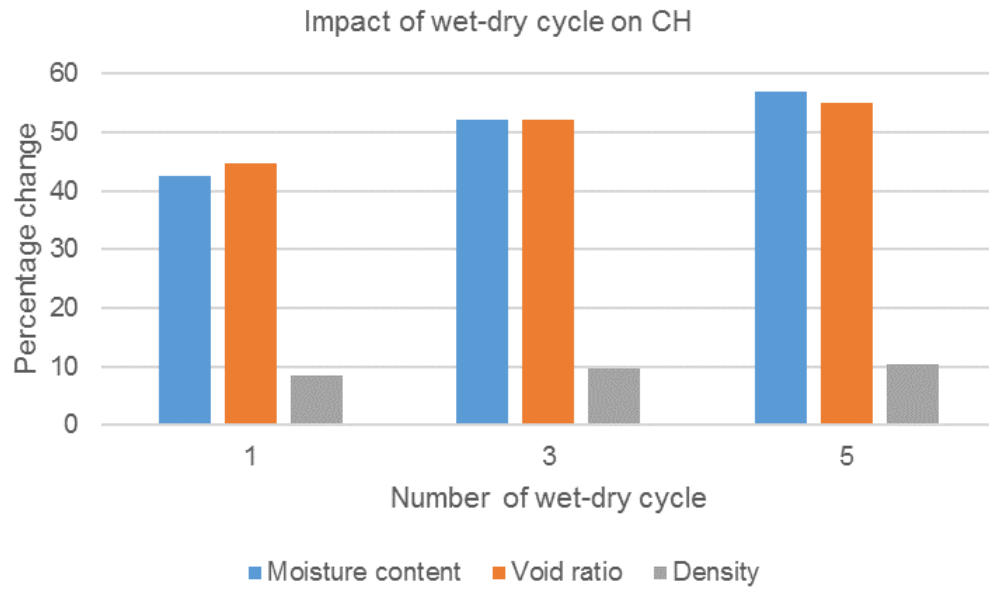


Figure 5-2 Impact of wet-dry cycle on physical properties of CH (LL=80) soil

Table 5-2 Impact of wet-dry cycle on mechanical properties of CH (LL =80) soil

W-D Cycle	c	ϕ
0	4.50	28.81
1	3.58	25.41
3	2.50	24.23
5	2.08	23.02

5.2 Recommendation for Future Studies

Impact of wet-dry cycle was observed for two different liquid limits. Both types of soil showed reduction of shear strength with the increasing number of wet dry cycle. Soils with different liquid limit may be used for further analysis to observe the impact. In this research, fully softened shear strengths were determined at low stress level and the observed angle of internal friction was found much less than the prediction from proposed correlation by Stark and Hussain (2013). Based on this research, recommendations for the future studies are summarized below:

- I. Impact of wet-dry cycle should be evaluated for different liquid limit of soil
- II. To observe the impact of boundary condition of the sample, different diameter and shape of samples should be prepared for direct shear testing
- III. Fully softened friction angle should be determined at low normal stress (< 50 kPa) with soil having different liquid limits to propose a correlation at shallow slope stability analysis
- IV. Monitoring the in situ density and moisture content within a slope up to a certain depth will provide an idea about the stability of the slope

References

Abramson, L., Lee, T., Sharma, S., and Boyce, G., (2002). Slope Stability and Stabilization Methods, John Wiley, New York, 712 p.

Abrams, T. G., & Wright, S. G. (1972). A SURVEY OF EARCH SLOPE FAILURES AND REMEDIAL MEASURES IN TEAXS (No. CFHR 3-8-71-161-1 Intrm Rpt.).

Al Zubaydi, A. T. (2011). Swell Potential, Collapse Potential, Wetting and Drying Cycles, Cracks, Number of Segment. Tikrit Journal of Engineering Science (TJES), 18(4), 71-79.

ASTM. 1963 (Reapproved 2002). "Designation D 422-63, Standard Test Method for Particle- Size Analysis of Soils." American Society for Testing and Materials, Philadelphia.

ASTM. 2000. "Designation D 698-00a, Standard Test Methods for Laboratory Compaction Characteristics of Soil Using Standard Effort (12,400 ft-lbf/ft³ (600 kN-m/m³))." American Society for Testing and Materials, Philadelphia.

ASTM. 2002. "Designation D 854-02, Standard Test Methods for Specific Gravity of Soil Solids by Water Pycnometer." American Society for Testing and Materials, Philadelphia.

ASTM. 2002. "Designation D 1557-02, Standard Test Methods for Laboratory Compaction Characteristics of Soil Using Modified Effort (56,000 ft-lbf/ft³ (2,700 kN-m/m³))."

ASTM. 2005. "Designation D 4318-05, Standard Test Methods for Liquid Limit, Plastic Limit, and Plasticity Index of Soils." American Society for Testing and Materials, Philadelphia

Bishop AW, Henkel DJ (1962) The measurement of soil properties in the triaxial test, 2nd Ed. Edward Arnold, London

Castellanos, B. A., Brandon, T. L., & VandenBerge, D. R. (2015). Use of fully softened shear strength in slope stability analysis. *Landslides*, 1-13.

Castellanos, B. A. (2014), *Use and Measurement of Fully Softened Shear Strength*. Ph.D. dissertation, Virginia Polytechnic Institute and State University

Chandler RJ, Pachakis M, Mercer J, Wrightman J (1973) Four long-term failures of embankments founded on areas of landslip. *Q J Eng Geol* 6:405–422.

Gamez, J. A., & Stark, T. D. (2014). Fully softened shear strength at low stresses for levee and embankment design. *Journal of Geotechnical and Geoenvironmental Engineering*, 140(9)

Gregory, G. H., & Bumpas, K. K. (2013). Post-peak fully-softened strength and curved strength envelope in shallow slope failure analysis. In *Geo-Congress 2013: Stability and Performance of Slopes and Embankments III* (pp. 255-268). ASCE.

Sayem Hossain Md, Kong Ling-wei, Yin Song. Effect of Drying-Wetting Cycles on Saturated Shear Strength of Undisturbed Residual Soils. *American Journal of Civil Engineering*. Vol. 4, No. 4, 2016, pp. 159-166. doi: 10.11648/j.ajce.20160404.15

Kenney, T. C. (1967). "The influence of mineral composition on the residual strength of natural soils." *Proc., Geotech. Conf., Norwegian Geotechnical Institute, Oslo, Norway*, 1, 123–129.

Loehr, J.E., and J.J. Bowders (2007), "Slope Stabilization Using Recycled Plastic Pins – Phase III," Research Report RI98-007D, Prepared for the Missouri Department of Transportation, 289 p.

Lade, P. V. (2010). "The mechanics of surficial failure in soil slopes." *Engineering Geology*, 114(1-2), 57–64.

Lupini, J. F., Skinner, A. E., and Vaughan, P. R. (1981). "The drained residual strength of cohesive soils." *Géotechnique*, 31(2), 181–213.

Mitchell, J. K. (1993). *Fundamentals of soil behavior*, 2nd Ed., Wiley, New York.

Pradel, D., & Raad, G. (1993). Effect of permeability on surficial stability of homogeneous slopes. *Journal of Geotechnical Engineering*, 119(2), 315-332

Rogers, L.E. and Wright, S.G. (1986). *The effects of wetting and drying on the long-term shear strength parameters for compacted Beaumont clay*. Center for Transportation Research, The University of Texas at Austin, Texas

Skempton, A. W. (1954). "The pore-pressure coefficients A and B." *Géotechnique*, 4(4), 143–147.

Skempton, A. W. (1964). "Long-term stability of clay slopes." *Géotechnique*, 14(2), 77–102.

Skempton, A. W. (1970). "First-time slides in over-consolidated clays." *Géotechnique*, 20(3), 320–324.

Stark, T. D., & Eid, H. T. (1997). Slope stability analyses in stiff fissured clays. *Journal of Geotechnical and Geoenvironmental Engineering*, 123(4), 335-343

Stark, T. D., Choi, H., & McCone, S. (2005). Drained shear strength parameters for analysis of landslides. *Journal of Geotechnical and Geoenvironmental Engineering*, 131(5), 575-588.

Stark, T. D., and Hussain, M. (2013). "Empirical Correlations: Drained Shear Strength for Slope Stability Analyses." *Journal of Geotechnical and Geoenvironmental Engineering*, 139(6), 853–862.

Titi, H., & Helwany, S. (2007). Investigation of Vertical Members to Resist Surficial Slope Instabilities (No. WHRP 07-03). Wisconsin Department of Transportation, Madison, WI.

VandenBerge, D. R., Duncan, J. M., & Brandon, T. L. (2013). Fully softened strength of natural and compacted clays for slope stability. In Geo-Congress 2013: Stability and Performance of Slopes and Embankments III (pp. 221-233). ASCE.

Wright, G. S., Zomberg G., and Aguetant, J. E. (2007). *The Fully Softened Shear Strength of High Plasticity Clays*. Texas Department of Transportation, Research and Technology Implementation Office.

Biographical Information

Md Ashrafuzzaman Khan was born in Dinajpur, Bangladesh on November 25, 1987. He graduated with a Bachelor of Science in Civil Engineering from Bangladesh University of Engineering and Technology, Dhaka, Bangladesh in February, 2011. After graduation, he joined JPZ Consulting Bangladesh as a junior design engineer. He also worked as a Lecturer in the department of civil engineering of Stamford University Bangladesh from January 2012 to July 2014. He started his graduate studies in the University of Texas at Arlington from Fall 2014. During his study he also got the opportunity to work as a Graduate Research Assistant under the supervision of Dr. Sahadat Hossain. The author's research interests include, slope stability analysis, stability of retaining structures, geophysical investigation with Resistivity Imaging and numerical modeling.